

GEOLOGY, ALTERATION, AND MINERALIZATION OF THE
RED MOUNTAIN STOCK, GRIZZLY PEAK
CAULDRON COMPLEX, COLORADO

By

MARK JOHN HOLTZCLAW
//

Bachelor of Science

Oklahoma State University

Stillwater, Oklahoma

1971

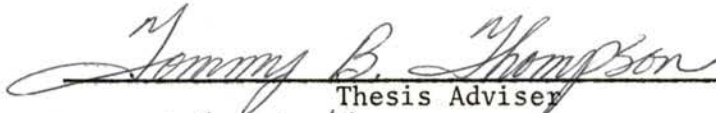
Submitted to the Faculty of the Graduate College
of the Oklahoma State University
in partial fulfillment of the requirements
for the Degree of
MASTER OF SCIENCE
May, 1973

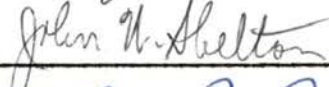
Thick
1975
H. 7559
CPT 5


OCT 8 1973


GEOLOGY, ALTERATION, AND MINERALIZATION OF THE
RED MOUNTAIN STOCK, GRIZZLY PEAK
CAULDRON COMPLEX, COLORADO

Thesis Approved:


Thesis Adviser






Dean of the Graduate College

PREFACE

The Grizzly Peak volcanic field, Colorado, occupies an area of approximately 50 square miles, exhibiting a somewhat circular configuration elongated along a northeasterly trend. Two recent studies evince the volcanic pile is associated with a mid-Tertiary cauldron complex. The purpose of this thesis is to investigate the geology, alteration, and mineralization of a ring-fracture intrusion along southern extremities of the central cauldron block.

Fieldwork for this study was initiated in late May of 1971 and completed by mid-July of the same year. Mapping was done on United States Forest Service aerial photographs enlarged to the scale of 1:6,350. Geologic data were transferred to a base map and reduced to the scale of 1:7,200. Rock samples were collected from most outcrops and subjected to rapid chemical analysis for molybdenum, tungsten, copper, lead, and zinc. Additional investigations include the following:

- 1) Detailed examination of 45 thin sections.
- 2) X-ray diffraction analysis, with particular emphasis on alteration minerals.
- 3) Whole rock major element analysis for a total of eight samples.

The author gratefully acknowledges the guidance of Dr. Tommy B. Thompson, thesis adviser. Professors John W. Shelton and Alex B. Ross, committee members, as well as Drs. Zuhair Al-Shaieb, Gary F. Stewart, Lester W. Reed, and Horacio A. Mottola, have all been generous with their time and constructive criticism. Their individual efforts are much

appreciated.

Generous financial assistance was received from Bear Creek Mining Company for chemical analyses and preparation of thin sections. Special appreciation is due to John and Darlene Holtzclaw for financing the major portion of this thesis. Most of all, the author wishes to thank his wife, Linda "Goose", for her patience and continual reassurance during the past two exceedingly trying years.

TABLE OF CONTENTS

Chapter	Page
I. ABSTRACT	1
II. INTRODUCTION	2
Location, Accessibility, and Topography	2
History of Mining and Development	3
III. GRIZZLY PEAK VOLCANIC FIELD: GENERAL STATEMENT.	6
IV. GEOLOGY OF THE RED MOUNTAIN AREA	9
Precambrian Rocks	10
Sawatch Schist and Migmatite	10
Quartz Biotite Monzonite	11
Tertiary Rocks.	12
Grizzly Peak Volcanics	12
Ash-Flow Tuffs.	12
Slump Breccias.	19
Andesite Porphyry Dikes.	20
Quartz Latite Porphyry Stock	22
Quartz Latite Porphyry Dikes	25
Intrusive Breccia Dikes.	30
Dacite Porphyry Dikes.	32
Rhyolite Porphyry Dikes.	34
Precambrian Structure	35
Tertiary Structure.	35
Igneous Rocks.	35
Fractures.	36
Faults	37
V. MINERALIZATION	40
Stockwork Mineralization.	41
Trace Element Study	43
Methods of Sampling and Analytical Analysis.	44
Background and Threshold Values.	44
Trace Element Distribution Maps.	48
Correlation Coefficients	49
Discussion of Stockwork Mineralization.	49

Chapter	Page
VI. ALTERATION	53
Hydrothermal Alteration Associated With Stockwork	
Mineralization.	55
Procedure.	55
Sericitic Zone	56
Silicified Zone.	56
Intermediate Argillic Zone	58
Less-Intense Argillic Zone	58
Discussion	62
Supergene Alteration.	63
VII. SUMMARY.	66
REFERENCES CITED.	71
APPENDIX A.	74
APPENDIX B.	76

LIST OF TABLES

Table	Page
I. Modal Analyses of Rhyolitic Ash-Flow Tuffs . . . ,	15
II. Modal Analyses of Quartz Latite Porphyry Dikes	27
III. Data Description of Trace Element Values From Selected Samples of Ash-Flow Tuff . , . . . ,	45
IV. Data Description of Trace Element Values From All Rock Types and Quartz Latite Porphyry Stock	47
V. Correlation Coefficient Matrices for Trace Element Values. . .	50
VI. Major Element Analyses	75
VII. Trace Element Analyses	77

LIST OF FIGURES

Figure	Page
1. Location Map	4
2. Generalized Geologic Map of Central Colorado	7
3. Geologic Map of Thesis Area.	In Pocket
4. Photograph of Ash-Flow Tuff Showing Compactional Layering	14
5. Photomicrograph of a Densely Welded Crystal-Rich Rhyolitic Ash-Flow Tuff.	16
6. Photomicrograph of a Densely Welded Ash-Flow Tuff Displaying Compactionally Layered Groundmass of Sub-Oriented Vitric Shards Interstratified With Comminuted Glass Particles and Pumice	18
7. Photomicrograph Showing the Devitrification of a Crushed Pumice Fragment in Ash-Flow Tuff	18
8. Photograph of Slump Breccia.	20
9. Photograph Showing Characteristics of the Quartz Latite Porphyry Stock	23
10. Photomicrograph of a Typical Quartz Phenocryst in the Quartz Latite Porphyry Stock	24
11. Photograph Showing Contact Relationships of a Quartz Latite Porphyry Dike	26
12. Photomicrograph of a Typical Quartz Phenocryst in a Quartz Latite Porphyry Dike.	28
13. Photomicrograph of a Biotite Crystal in Quartz Latite Porphyry Dike.	30
14. Photograph Showing Fragmental Characteristics of the Intrusive Breccia Dikes.	31
15. Photomicrograph Showing Characteristics of Dacite Porphyry Dike.	33

Figure	Page
16. Photomicrograph of a Zoned Plagioclase Lath in Dacite Porphyry Dike,	33
17. Generalized Cross Sections Through Red Mountain,	38
18. Photograph of an Unusually Well Developed Polymetallic Sulfide Vein,	41
19. Photograph Showing Stockwork Veinlets,	43
20. Index Map to Sample Locations,	In Pocket
21. Trace Element and Alteration Distribution Maps	In Pocket
22. Red Mountain Looking South Along the Continental Divide, .	54
23. Photomicrograph of an Altered Plagioclase Phenocryst From Sericitic Alteration Zone of the Red Mountain Stock,	57
24. Photomicrograph of an Altered Biotite Crystal From Sericitic Alteration Zone of the Red Mountain Stock, . .	57
25. Photomicrograph of an Altered Plagioclase Lath From Intermediate Argillic Alteration Zone of the Red Mountain Stock,	59
26. Photomicrograph of an Altered Biotite Crystal From Intermediate Argillic Alteration Zone of the Red Mountain Stock,	59
27. Photograph Showing Progressive Degree of Hydrothermal Bleaching in Ash-Flow Tuff Toward the Red Mountain Stock,	60
28. Photomicrograph of an Altered Plagioclase Crystal From Less-Intense Argillic Alteration Zone of Ash-Flow Tuff,	61
29. Photomicrograph of an Altered Biotite Crystal From Less- Intense Argillic Alteration Zone of Ash-Flow Tuff, . . .	61
30. Photograph Showing Typical Surface Colors Expressed at Red Mountain,	64

CHAPTER I

ABSTRACT

Crystal-rich rhyolitic ash-flow tuffs, slump breccias, intrusive breccias, two dike sets, and a quartz latite porphyry stock are revealed in the Red Mountain area of the Grizzly Peak cauldron complex, Colorado. Various geologic relationships indicate the area is within a poorly defined southern ring-fracture zone of the central cauldron block.

Two major hydrothermal events of mid-Tertiary age are recorded in the Tertiary rocks at Red Mountain. The first event is evidenced in a quartz-pyrite-molybdenite stockwork and four distinct, pervasive, and somewhat systematic zones of hydrothermal alteration--all genetically associated with the quartz latite stock. A second and younger hydrothermal event is revealed laterally away from the stockwork in polymetallic sulfide veins along N65E-N80E-trending fractures. The relative age of these latter veins is clearly shown by their spatial association with "late" rhyolite dikes. Crosscutting relationships provide evidence of a cyclic magmatic-hydrothermal history, reflecting physical and chemical changes within a single master magma reservoir.

Supergene alteration, although markedly displayed in surface colors, is not strongly developed in the Red Mountain area. The topographic relief, recent glaciation, dry cool climate, and geologic youth have restricted chemical weathering to the very near surface environment.

CHAPTER II

INTRODUCTION

The Sawatch Range of central Colorado is a northwest trending uplift eroded to expose a core of Precambrian metasedimentary rocks and granitic bodies. South of Independence Pass, these Precambrian rocks are unconformably overlain by intermediate to acidic ash-flow tuffs of the Grizzly Peak volcanic field. Recent investigations by Candee (1971b) and Cruson (1972) reveal that the ash-flows ponded in a mid-Tertiary cauldron, together with large quantities of breccia derived from the cauldron walls. A partial recovery of initial magmatic pressure resulted in forceful injection of a central granodiorite stock doming overlying volcanics. Later eruptions of ash-flows were accompanied by partial collapse of a smaller cauldron overlapping southern extremities of the central cauldron block. Emplacement of porphyry stocks, plugs, and dikes occurred throughout development of the cauldron complex, particularly along southern ring-fracture zones. The objectives of this study are to investigate the geology, alteration, and mineralization of one such stock and contiguous rock units,

Location, Accessibility, and Topography

The thesis area, roughly two square miles, is focused over a resplendent ridge, appropriately known as Red Mountain. Geographically this mountain is situated on the Continental Divide in Pitkin and Chaffee

Counties, approximately 20 miles southeast of Aspen, Colorado (Fig. 1). The area lies in the southwestern quarter of the Independence Pass quadrangle, between longitude $106^{\circ}37'00''$ and $106^{\circ}34'30''W$ and latitude $39^{\circ}02'00''$ and $39^{\circ}00'30''N$.

Access is possible by either the Lincoln Gulch Road or the South Fork of Lake Creek Road, both of which intersect Colorado Highway 82. The South Fork of Lake Creek Road is the better of the two, although vehicles with high ground clearance are recommended. The Lincoln Gulch Road requires four wheel drive from Grizzly Reservoir to Red Mountain, approximately six miles. Use of both access roads is limited to the summer months because of the extreme winters the vicinity experiences.

Regional topography is extreme with a maximum relief in excess of 4,000 feet to the north of Red Mountain. Elevations in the study area range from 11,000 feet in Lincoln Gulch to 13,640 feet at the summit of Red Mountain; timberline is at approximately 11,800 feet.

Many topographic features of the region are of glacial origin, such as U-shaped valleys, lateral moraines, cirques, and tarns. Red Mountain, as many neighboring peaks, appears rounded owing to Quaternary debris and a plethora of talus slopes. Knobs and ridges of bedrock piercing the Quaternary tegument give rise to a hummocky topography.

History of Mining and Development

References made to Red Mountain by O. J. Hollister (1867) indicate mining activities began in that area during the mid-1800's. To the present date, a great deal of prospecting but little production has resulted.

The Ruby Mine, owned and operated by the Ruby Mining and Development

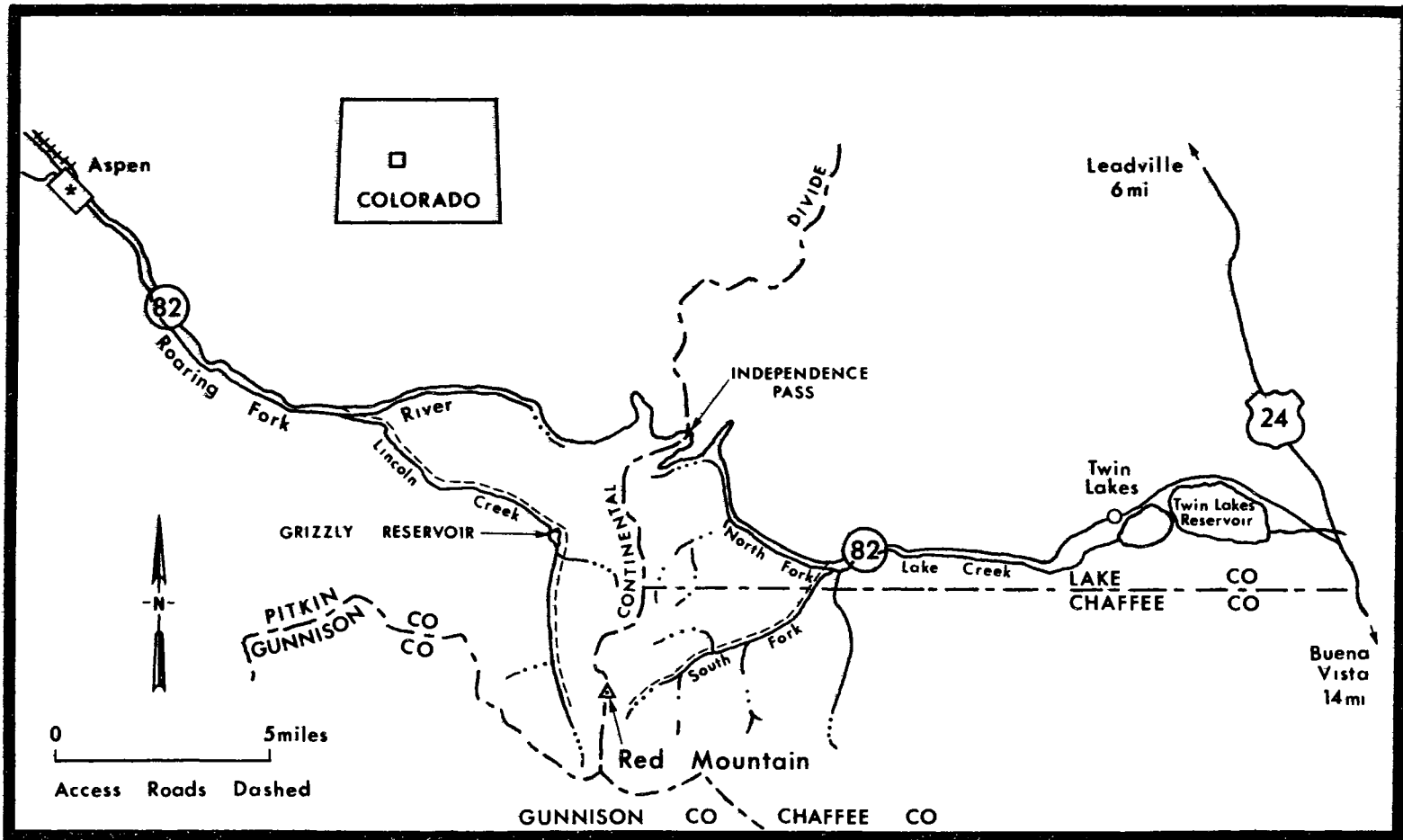


Figure 1. Location Map.

Company, was by far the largest operation in the area. The mine, reported to consist of 2,500 feet of tunnel and drifts, was worked sporadically from 1905 through 1929. Ore was concentrated in a 50-ton plant erected at the mine in 1906. Production figures were not available; however, Mineral Resources of the United States Reports indicate small but high-grade lots of gold-silver bearing zinc-copper-lead ore were shipped to the Leadville smelter during the years 1906, 1907, 1908, 1911, and 1929 (Naramore, 1906, 1907; Henderson, 1908, 1911, 1929).

The only other significant activity occurred in Peek-a-boo Gulch from the early 1900's to 1941 at a group of prospects known collectively as the Anchor Group Mines. The only recorded production was in 1941 when two tons of ore, yielding one ounce of gold and one and one-half ounces of silver per ton, were shipped to the Golden Cycle Mill (Vanderwilt, 1947). Harsh weather, isolation, and lack of economic ore terminated mining activities in the Red Mountain area.

In 1919, J. V. Howell observed molybdenite at Red Mountain and stated:

The veins in the vicinity of Red Mountain which carry molybdenite are always so closely associated with Red Mountain rhyolite that it appears nearly certain that the flow is the source of the mineral. Molybdenite is disseminated in the rhyolite itself, along with finely disseminated pyrite.

Interest in Red Mountain as a possible molybdenite deposit has resulted in the completion of exploratory drilling programs by a number of companies. Unfortunately, results are not made available for this thesis.

CHAPTER III

GRIZZLY PEAK VOLCANIC FIELD: GENERAL STATEMENT

The Grizzly Peak volcanic field occupies an area of approximately 50 square miles, exhibiting a somewhat circular configuration elongated along a northeasterly trend (Fig. 2). Two recent studies evince the volcanic sequence is associated with a mid-Tertiary cauldron complex. The more recent and comprehensive of these studies was conducted by Cruson (1972), who states:

The Grizzly Peak cauldron complex is associated with early Oligocene exotic breccias and intermediate to acidic ash-flow tuffs that occur both within and immediately outside the complex. It occupies 128 square kilometers and contains screen, intrusives, differentially subsided blocks, volcanic necks and domes, breccia pipes, pyroclastic dikes, and hydrothermal stockworks. Fifteen hundred meters of interstratified breccias and tuffs are preserved in areas of maximum subsidence.

Structural development began with the collapse of a circular central block 8.5 km. in diameter. Ash-flow tuffs ponded in the cauldron, together with large quantities of breccia shed from the walls. Resurgence resulted in a central granodiorite intrusive that domed overlying welded ash-flows. Later eruptions of rhyolitic ash-flows were accompanied by subsidence of a smaller cauldron south of the central block which partially collapsed and overlapped the earlier cauldron.

Several andesitic to rhyolitic magmatic events are recorded in concentric dike systems and plugs. Younger quartz latite intrusives are associated with multiple hydrothermal events that resulted in molybdenum and gold-silver mineralization.

Candee (1971) has completed a study of the central granodiorite intrusive (Lincoln Gulch Stock) and states:

The main rock type of the stock is a magnetite-bearing biotite granodiorite porphyry with zoned plagioclase feldspar and euhedral beta quartz phenocrysts. The United States Geological Survey has dated the Lincoln Gulch Stock as 33.9

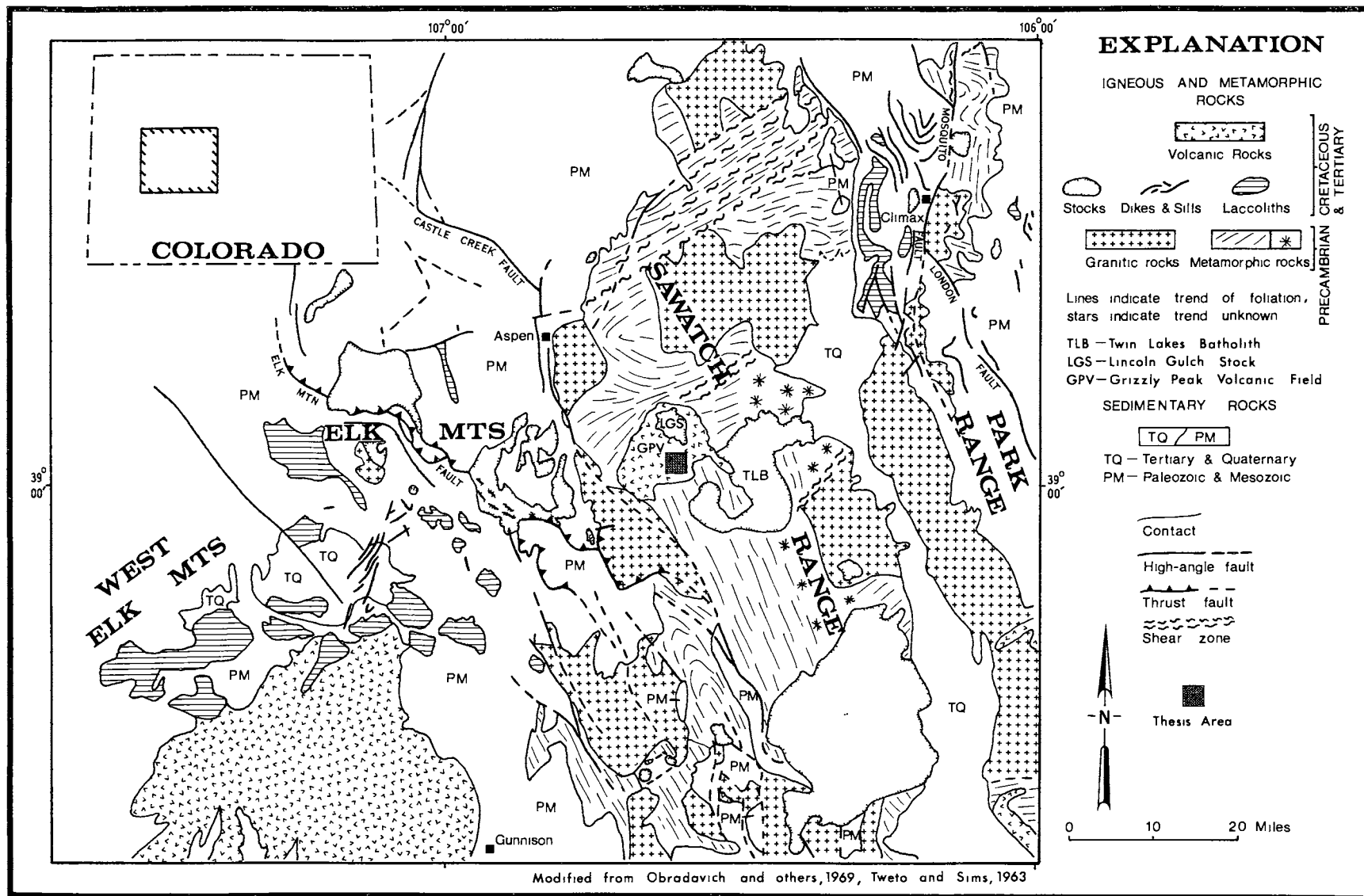


Figure 2. Generalized geologic map of Colorado.

million years. The outline of the stock is roughly rectangular, with the long dimension being 3.2 miles in a northwesterly direction and 2.3 miles wide in the northeasterly direction. The contacts are generally sharp and dip toward the center of the stock; but the northeast contact dips away to the northeast at approximately 45 degrees. Numerous xenoliths of Precambrian gneiss and schist and rare xenoliths of ash-flow tuffs and the Twin Lakes Granodiorite (?) are found in the stock. The stock has intruded and domed approximately 3,000 feet of interlayered ash-flow tuffs and slump-breccias, which fill a cauldron (?) subsidence structure. Dikes of latitic and dacitic composition have intruded both the stock and volcanic sequence. The whole area has then been faulted by steeply dipping N20W and N45W trending fractures. Petrographic and chemical data suggest that the volcanics, stock, and later dikes represent a differentiation trend from rhyolite to dacite of a single magma chamber.

Candee observed that hydrothermal alteration and mineralization were primarily restricted to the southern ring-fault zone and related to a source postdating emplacement of the Lincoln Gulch Stock.

Prior to the investigations by Candee and Cruson, reconnaissance studies of limited significance were completed by Howell (1919), Vanderwilt and Koschman (1932), Stark and Barnes (1935), and Burbank and Goddard (1935). The K/Ar age date of 33.9 million years for the Lincoln Gulch Stock was determined by Obradovich and others (1969). In 1969, Lipman and others suggested the Grizzly Peak volcanic field was related to a Tertiary subsidence feature.

CHAPTER IV

GEOLOGY OF THE RED MOUNTAIN AREA

Red Mountain lies along the southern margin of the Grizzly Peak volcanic field, approximately one and one-half miles south of the resurgent Lincoln Gulch Stock. Various geologic relationships lead the author to conclude the area is within a poorly defined southern ring-fracture zone of the central cauldron block. Until Cruson's findings are published in full, however, the exact position of Red Mountain relative to the cauldron complex--as well as a final assessment of structural, magmatic, and hydrothermal events recorded at Red Mountain--cannot be ascertained without a moderate degree of uncertainty.¹

Relief in the Red Mountain area provides a composite 1,800 foot vertical section of interstratified ash-flow tuffs and slump breccias unconformably overlying a Precambrian basement of metasedimentary and igneous rocks. Intruding these country rocks are a quartz latite porphyry stock (referred to as the Red Mountain stock), intrusive breccias, and porphyry dikes of andesite, dacite, rhyolite, and quartz latite composition. A major hydrothermal event is recorded in a quartz-pyrite-molybdenite stockwork permeating the quartz latite porphyry stock. A second and later hydrothermal event is evidenced in polymetallic sulfide veins

¹Cruson presented his findings at the 68th Annual Meeting of the Geological Society of America. References to his work were taken from an abstract of a paper presented at that meeting. At the time of this publication, his dissertation was still in preparation.

occurring along fractures away from the stockwork and in close association with rhyolite porphyry dikes. A partial sequence as expressed by crosscutting relationships, alteration, and mineralization of the surface Tertiary rocks can be summarized as follows:

- youngest - (5) rhyolite porphyry dikes (Trp) $\begin{matrix} \uparrow \\ ? \\ \downarrow \end{matrix}$ polymetallic sulfide mineralization
- (4) dacite porphyry dikes (Tdp)
- (3) quartz-pyrite-molybdenite stockwork $\begin{matrix} \leftarrow ? \\ \leftarrow ? \end{matrix}$ intrusive breccia dikes (Tib)
- (2) quartz latite porphyry stock (Tqlp) $\begin{matrix} \leftarrow ? \\ \leftarrow ? \end{matrix}$ quartz latite porphyry dikes (Tqld)
- $\leftarrow ? \rightarrow$ andesite porphyry dikes (Tap)
- oldest - (1) crystal rich rhyolitic ash-flow tuffs (Tgpr) and interbedded slump breccias (Tgpb).

The reader should refer to the geologic map (Fig. 3) while reading this chapter. Other than in special cases, reference to the map will not be made in the remaining pages. Classification of rock types follows the scheme presented by Moorhouse (1959).

Precambrian Rocks

Sawatch Schist and Migmatite

The oldest rocks in the thesis area are Precambrian migmatized paragneisses referred to by Stark and Barnes (1935) as the Sawatch Schist and Migmatite. These metasedimentary rocks are exposed along the east side of Peek-a-boo Gulch; however, they are not readily distinguishable

on aerial photographs owing to the similar surface coloration of superjacent ash-flow tuffs.

White permatitic stringers, which parallel and are intermixed with intensely foliated schistose layers, characterize the Sawatch Schist and Migmatite. These lenses consist of large anhedral crystals of microcline in coextensive proportions with large anhedral grains of strained quartz. They are often connected by cross veins of the same material, stringers and veins alike blending without sharp contact into schistose layers.

Schistose layers are invariably dark green, consisting of oriented green biotite plates (partly chloritized), bladed crystals of sillimanite, anhedral grains of quartz, and clusters of euhedral pyrite cubes. Biotite occasionally displays a wedge-shaped form, the wide end of the wedge fraying out against other minerals.

Quartz Biotite Monzonite

Candee (1971) describes Precambrian quartz biotite monzonite stocks intruding the migmatized parashists of the Independence Pass vicinity. Outcrops of a similar rock are exposed north of the Ruby Mine on the northeastern flank of Red Mountain. For lack of contrary evidence, these outcrops are considered to represent an intrusion related to those described by Candee.

The quartz biotite monzonite is typically light gray, medium grained, and hypautomorphic-granular. Andesine (An_{30}), braded perthite, quartz, and microcline make up approximately 85 percent of the rock. The remainder consists of biotite, hornblende, magnetite, apatite, and sphene. Andesine occurs as euhedral to subhedral laths, separated from

one another by interstitial quartz and microcline. Braded perthite occurs as large anhedral crystals, often poikilitically enclosing euhedral crystals of plagioclase and hornblende. Biotite is typically present as subhedral plates which are chloritized along margins and cleavage planes. Euhedral apatite, subhedral sphene, and subhedral to anhedral magnetite crystals are abundant and occasionally occur as zonally arranged inclusions in the braded perthite.

Tertiary Rocks

Tertiary rocks of the Red Mountain area are described in the following pages in the order of their respective ages, starting with the oldest (see page 10). Sections on the andesite and quartz latite porphyry dikes respectively precede and follow discussion of the quartz latite porphyry stock; however, age relationships of these two intrusive phases relative to each other or the stock are not proven.

With exception of the quartz latite dikes, the porphyry intrusions have undergone pervasive deuteric and/or hydrothermal alteration. The effects of alteration, when coupled with a microcrystalline and largely indistinguishable groundmass, make rock types most difficult to determine. For these reasons, the mineralogical names applied to the porphyry intrusions are tentative and are based in part on pseudomorphic relationships.

Grizzly Peak Volcanics

Ash-Flow Tuffs. The term "ash-flow tuff" is used to denote effusive volcanic rocks resulting from the passage of nuee'ardentes. Synonymous terms in common use include "ignimbrite" and "welded tuff".

Emplacement of ash-flow tuffs in the thesis area occurred during several volcanic eruptions as evidenced in Lincoln Gulch by recurring interstratification of breccia units and ash-flows. No attempt was made to distinguish cooling units; therefore, no distinction will be made for ash-flows below, interlayered with, or above the breccia units.

The ash-flows typically appear dense, showing little or no internal structure. There are exceptions, however, as revealed along the northwestern flank of Red Mountain by intense compactional layering (eutaxitic structure) striking N60E and dipping 30 degrees toward the northwest (Fig. 4). Subdued compactional layering of similar strike but diminished dip is apparent along the ridge line both north and south of the Red Mountain stock.

The ash-flows are typically buff gray to grayish black, crystal rich, densely welded rhyolites. They contain phenocrysts, largely broken, of quartz, sanidine, anorthoclase, plagioclase, biotite, magnetite, and sphene, pumice lapilli and blocks, and allogenic fragments. Local variations in composition and degree of welding occur but not with any apparent vertical or horizontal trends. Modal and chemical analyses are presented respectively in Table I and Appendix A.

Quartz, sanidine, and anorthoclase occur as angular fragments or occasionally as fractured euhedral to subhedral phenocrysts up to 5mm in the longest dimension (Fig. 5). Quartz, the more abundant of the orthomagmatic crystals, displays sharp extinction and weak to moderate resorption. Sanidine exhibits a chatoyant luster, axial angles of ten degrees or less, and occasionally simple twinning according to Carlsbad law. Anorthoclase is distinguished by a blotchy extinction and axial angles of about 50 degrees. Sanidine and anorthoclase are weakly

sericitized, anorthoclase to a slightly more intense degree. Quartz is totally free of alteration.



Figure 4. Compactional layering in ash-flow tuff striking N60E and dipping 30° toward the northwest (hammer is 14 inches long).

TABLE I
 MODAL ANALYSES OF RHYOLITIC ASH-FLOW TUFFS

Constituents	Sample LG 76	LG 53	PG 58	PG 53
quartz	16.1	18.4	14.7	18.3
potassium feldspar ¹	10.5	13.0	10.1	12.7
plagioclase	4.2	3.7	5.3	2.9
biotite	2.1	3.4	4.1	2.2
opaques ²	1.3	1.2	0.9	1.7
lithic fragments	2.8	8.5	5.2	4.3
groundmass	62.4	47.2	52.8	52.3
Total %	99.4	99.9	99.6	99.7

¹Includes anorthoclase.

²Includes sphene.

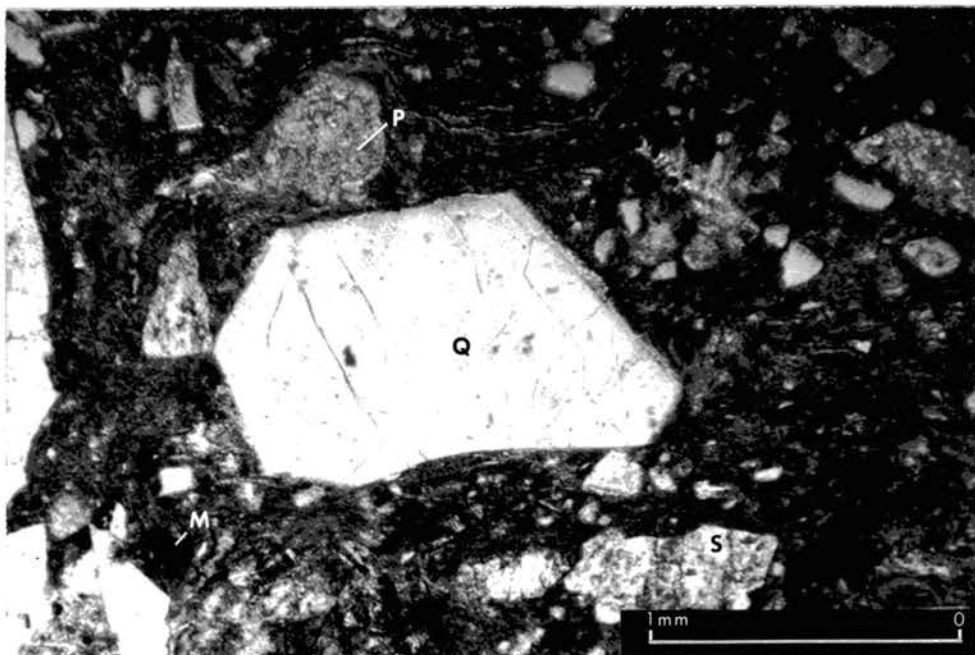


Figure 5. Photomicrograph of densely welded crystal-rich rhyolitic ash-flow tuff. Note weakly corroded quartz fragment in center of photograph (Q-quartz, S-sanidine, P-plagioclase, M-magnetite; crossed nicols).

Of the plagioclase minerals identified, only oligoclase appears indigenous to the ash-flows. Like other orthomagmatic crystals, it is typically fragmental, although occasionally occurs as fractured subhedral phenocrysts averaging 2mm in the longest dimension. Typical crystals are twinned according to the Carlsbad-albite laws, compositionally zoned outward, and masked by clay with disseminated grains of sericite. Degree of alteration is variable, but only rarely so intense as to impede optical measurements.

Biotite occurs as corroded euhedral to subhedral plates up to 2mm in length. Reaction rims of sericite mixed with lesser amounts of

chlorite are ubiquitous, extending inward along cleavage planes and fractures. Subhedral to anhedral magnetite crystals averaging 0.5mm across are typically enclosed in or are just marginal to the biotite plates. Sphene, which is almost always associated with magnetite and biotite, occurs as euhedral to anhedral crystals that average 0.1mm in length.

"Accidental" fragments of quartz, microcline, and occasionally braded perthite are apparent, commonly with bits of matrix adhering to them. Quartz invariably shows strong undulatory extinction, a feature which allows its distinction from fragmental quartz indigenous to the ash-flows. Other xenocrysts are easily distinguished by their optical characteristics.

Origin of the xenocrysts is well established as the ash-flows contain numerous xenoliths of quartz biotite monzonite. Boulders in excess of ten feet in diameter are common, especially in ash-flows at higher elevations. Occasionally, xenoliths of Sawatch Schist and Migmatite and ash-flow tuff are found.

The groundmass, which comprises between 45 and 60 percent of the ash-flow tuff, consists of vitric shards, pumice fragments, and comminuted glass particles. The matrix is typically dark gray, densely welded, unaltered, and weakly devitrified (Fig. 6). Vitric shards are intensely flattened and characteristically deflected around crystal fragments. Pumice fragments are crushed and drawn out, producing a eutaxitic texture. Most larger pumice fragments display interior zones of glass interlayered with lenticular lenses of microcrystalline quartz and feldspar (Fig. 7), features which undoubtedly represent devitrification.

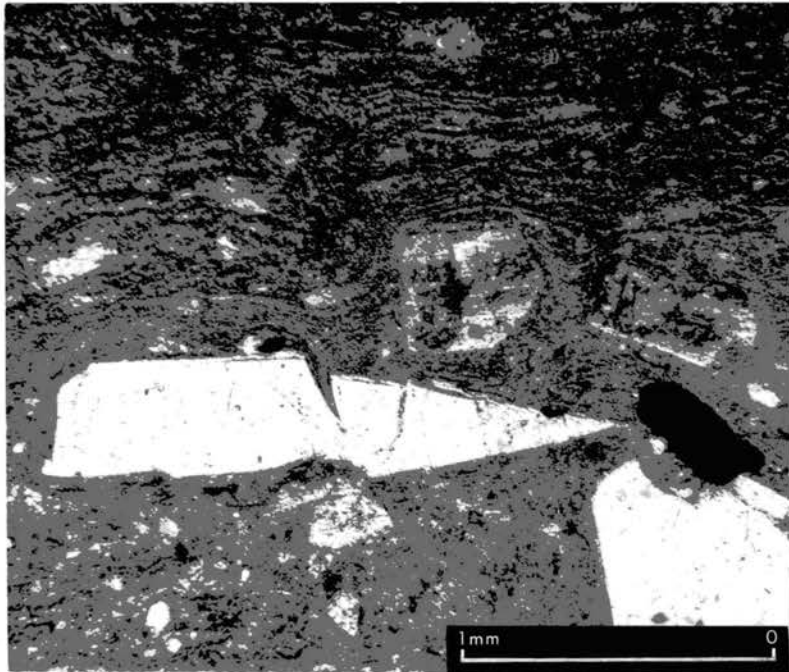


Figure 6. Photomicrograph of densely welded ash-flow tuff displaying compactionally layered groundmass of sub-oriented vitric shards interstratified with comminuted glass particles and pumice. Note shards are deflected around crystal fragments (ordinary light).

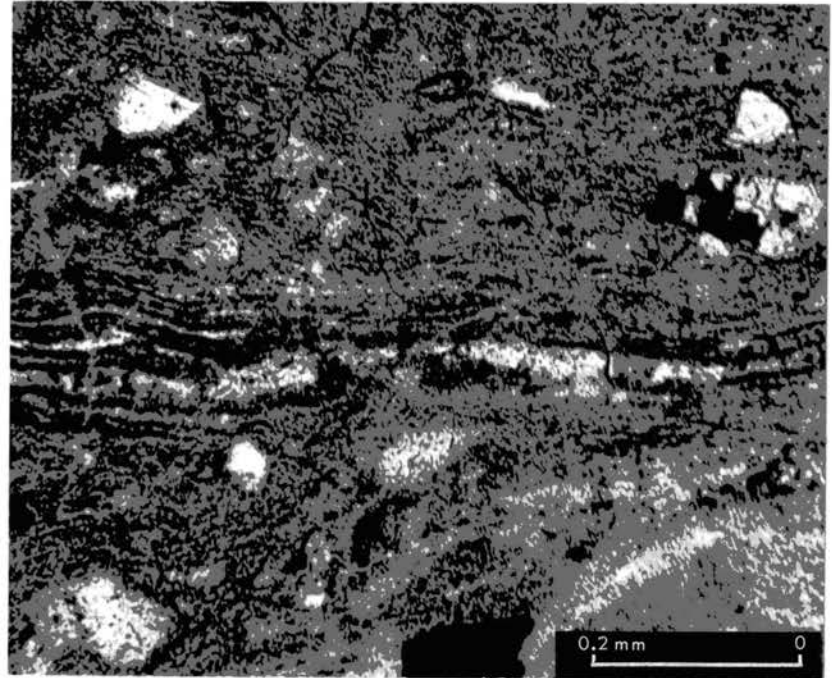


Figure 7. Photomicrograph showing devitrification of crushed pumice fragment. Interior zones consist of pumice interlayered with lenticular lenses of microcrystalline quartz and feldspar (ordinary light).

Slump Breccias. This term is used to describe breccias which formed as the result of gravity slides off the cauldron walls. As such, they are superjacent formations on the subsided cauldron floor. Candee (1971) and Cruson (1972) established the occurrence of these exotic breccias in the Grizzly Peak cauldron complex.

Slump breccias are exposed in the gulches east and west of the Continental Divide from Grizzly Peak southward to Red Mountain. Relief in Peek-a-boo Gulch provides an 800 foot vertical section of exposed breccia, whereas vertically recurring wedges of breccia interstratified with thin ash-flow sheets are exposed in Lincoln Gulch. Westward thinning and vertical repetition suggest emplacement occurred during stages from an easterly direction.

The breccias consist of angular to subangular blocks of granitic and metamorphic rock set in a silicified and comminuted matrix of the same (Fig. 8). Sorting is poor as fragments range from minute grains to boulders in excess of ten feet in diameter. Indeterminate combinations of iron oxides and ferric hydroxides are ubiquitous, staining fragments and matrix alike. Thin section studies evince angular fragments of quartz biotite monzonite, Sawatch Schist and Migmatite, and rarely, rhyolitic ash-flow tuff set in a silicified matrix of crushed rock. Alteration of the fragments is surprisingly minor considering the extensiveness of hematitic and limonitic staining. Plagioclase is typically masked by clay minerals enclosing disseminated grains of sericite. Biotite is usually chloritized, occasionally sericitized. Total transformation of magnetite to hematite is common but not pervasive. Quartz and potassium feldspar display an absence of alteration.



Figure 8. Photograph of slump breccia containing angular to subangular blocks of granitic and metamorphic rock set in a silicified and comminuted matrix of the same constituents (hammer is 14 inches long). Coloration result of indeterminate combinations of iron oxides and ferric hydroxides.

Andesite Porphyry Dikes

An andesite porphyry dike with a northwest trending arcuate trace (concave to the south) is exposed north of the Red Mountain stock. A second dike is revealed west of the stock, aligning with western exposures of the arcuate dike. Although there is no conclusive evidence, the author suspects both exposures are of the same dike. The dikes, or dike as the case may be, are approximately 5 feet wide, display sharp contacts with the country rock, and exhibit a moderate degree of resistivity to weathering.

The andesite appears intensely propylitized, displaying large phenocrysts of altered feldspar set in a dark green aphanitic groundmass. Extreme effervescence in hydrochloric acid shows large quantities of calcium carbonate--a characteristic which distinguishes the rock from any other in the Red Mountain area.

Thin section studies reveal phenocrysts of saussuritized plagioclase, chloritized biotite, and magnetite set in a microcrystalline matrix of altered feldspar. There is some quartz, but it is confined to the groundmass and several small veinlets. No potassium feldspar was observed. Petrographic studies indicate 57 percent is groundmass with remaining phenocrysts in the following "approximate" proportions: 35 percent plagioclase, 5 percent biotite, and 3 percent magnetite.

Mixtures of calcite, chlorite, and montmorillonite(?) have totally replaced all plagioclase phenocrysts. These pseudomorphs retain the euhedral to subhedral form, ranging from 1mm to 8mm and averaging 3mm in the longest dimension. Many display relicts of polysynthetic twinning. Most enclose euhedral to subhedral crystals of unaltered apatite.

Biotite is totally replaced by chlorite exhibiting a "Berlin blue" interference color. These pseudomorphs retain a euhedral form, ranging from 0.5mm to 2mm in length, averaging 1mm. In many instances, small anhedral grains of magnetite are apparent along margins and cleavage planes.

The matrix is microcrystalline, consisting of partly altered feldspar and lesser amounts of quartz. Aggregates of interlocking "flake-like" chlorite crystals occur throughout. These aggregates occasionally contain anhedral grains of magnetite, partly altered to hematite.

Quartz Latite Porphyry Stock

The Red Mountain stock has a rectangular configuration elongated some 4,000 feet along a N20W trend, varying from 1,000 to 2,000 feet in width. Most of the stock lies west of the Continental Divide on the southwestern flank of Red Mountain between the elevations of 12,400 and 13,200 feet. The ubiquity of limonitic staining, extensive deposits of Quaternary debris, and the rock's low resistivity to weathering prohibit an easy distinction of outcrops. Contact relationships of the stock and contiguous volcanic units were not observed. In order to show control, outcrops are included on the otherwise interpretive geologic map (Fig. 3).

Samples from outcrops in the northern, central, and southwestern areas of the stock have undergone intense hydrothermal alteration--to the extent that all preexistent textures and most orthomagmatic minerals are destroyed. These rocks are characterized by "squared" phenocrysts of quartz (prismatic orientation) and quartz-molybdenite-pyrite veins, all set in a light gray groundmass of coarse sericite intermixed with small anhedral crystals of quartz and disseminated grains of pyrite (Fig. 9, left sample).² Other than relicts of polysynthetic twinning, all traces of feldspar are absent. Biotite has been totally replaced by a mixture of muscovite, rutile, and pyrite. No magnetite was observed in any of these samples.

²Distinction of these "quartz-sericite-pyrite" rocks as being part of a stock rather than altered ash-flow tuffs is based on the following: (1) "squared" quartz phenocrysts are not observed in the ash-flows; (2) eutaxitic texture is revealed in the most intensely altered ash-flows; (3) distribution of these rocks occurs along a N20W trend, paralleling other porphyry intrusions.

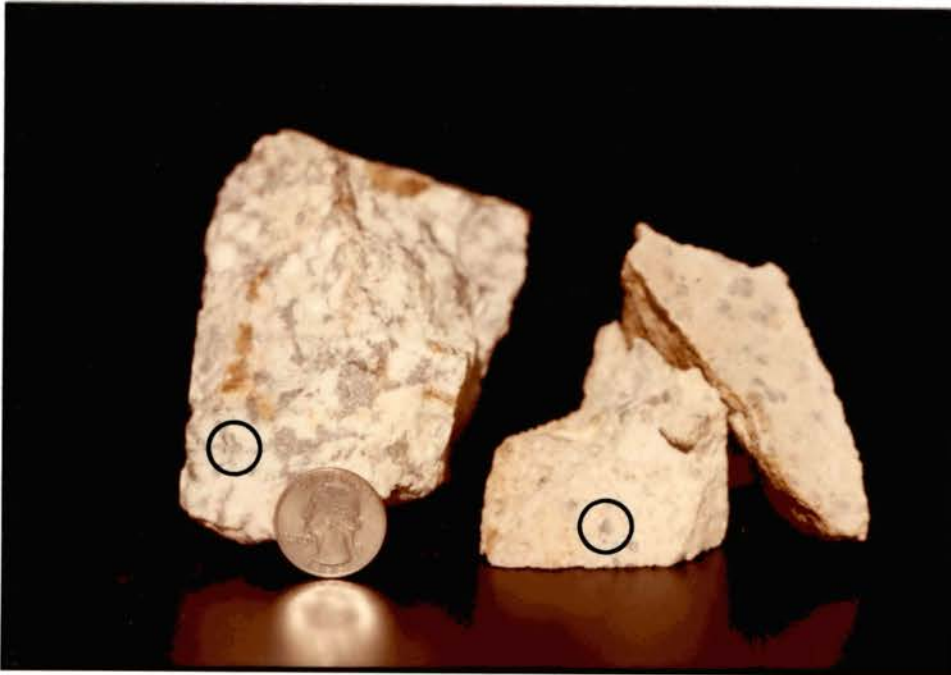


Figure 9. Photograph displaying characteristics of the quartz latite porphyry; sample on left characterizes outcrops from northern and central areas of the stock, sample on right characterizes outcrops from marginal areas of the stock. Note "squared" quartz phenocrysts in both samples.

Samples from the western and southeastern margins of the stock are likewise intensely altered but retain many preexistent textural and mineralogical characteristics. These samples are characterized by phenocrysts of quartz, altered plagioclase, partly altered potassium feldspar, and altered biotite, all set in a light gray to pinkish gray aphanitic groundmass (Fig. 9, right sample). Petrographic studies indicate 64 percent is groundmass with remaining phenocrysts in the following "approximate" proportions: 15 percent plagioclase, 11 percent quartz, 7 percent potassium feldspar, 3 percent biotite. Chemical analyses for these rocks, as well as for the intensely altered rocks, are presented in Appendix A.

Quartz phenocrysts occur as euhedral to anhedral crystals ranging from 2mm to 6mm and averaging 3mm in the longest dimension. Many of the crystals are bipyramidal, appearing as squares when broken along their C-crystallographic axes. Crystals are usually fractured, intensely corroded, and embayed (Fig. 10). Quartz displays an absence of undulatory extinction and sericitization.

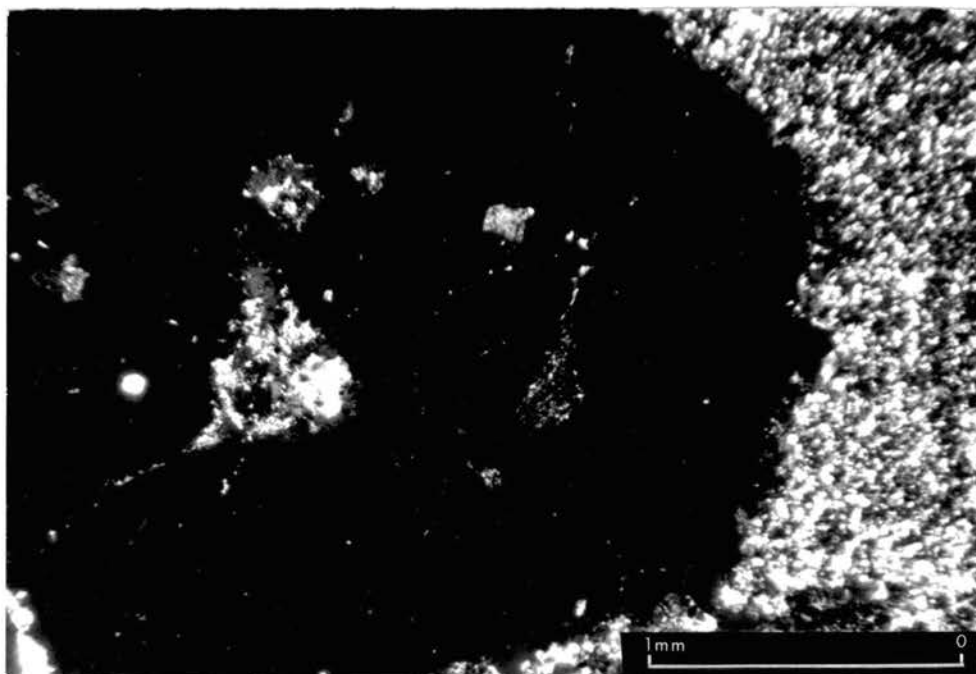


Figure 10. Photomicrograph of quartz phenocryst set in a microcrystalline and indistinguishable groundmass of quartz and altered feldspar; sample taken from a southern exposure of the stock. Note euhedral form, fractures, corrosion and penetration by lobes of matrix (crossed nicols).

Potassium feldspar phenocrysts occur as anhedral crystals ranging from 2mm to 5mm and averaging 3mm in the longest dimension. Studies

indicate 2V measurements on the order of 30 degrees--indicative of disordered orthoclase (Barth, 1969). Transformation to sericite is usually well developed along fractures and crystal margins, extending inward to a thin mask of disseminated grains.

Mixtures of sericite and clay have totally replaced all plagioclase phenocrysts. The pseudomorphs retain a euhedral to anhedral form, ranging from 1mm to 6mm averaging 3mm in the longest dimension. Many display relicts of polysynthetic twinning.

Biotite crystals have been altered to muscovite pseudomorphs entwining cleavage-oriented grains and lenses of rutile and pyrite. These pseudomorphs retain a euhedral to subhedral form ranging 0.5mm to 3mm and averaging 1mm in length. In many cases, they display preexistent resorption textures. Occasionally, they poikilitically enclose small euhedral to anhedral crystals of unaltered sphene.

The matrix is microcrystalline-equigranular, consisting of indeterminate amounts of quartz and altered feldspar. The grain size approximates 0.05mm although occasionally it is slightly coarser.

Quartz Latite Porphyry Dikes

Quartz latite porphyry dikes with trends varying between N20W and N65W intrude the ash-flow tuffs along the northern and western flanks of Red Mountain. The dikes range from 5 to 20 feet in width, display sharp contacts with chilled margins (Fig. 11), and exhibit a high degree of resistivity to weathering.

The quartz latite appears unaltered in hand sample, displaying large crystals of quartz, feldspar, magnetite, and "book" biotite set in a light gray aphanitic groundmass. Thin section studies indicate a

glomeroporphyritic fabric--the only significant characteristic distinguishing textures and mineralogy of the dikes from those implied in the quartz latite porphyry stock. Modal and chemical analyses are presented respectively in Table II and Appendix A.

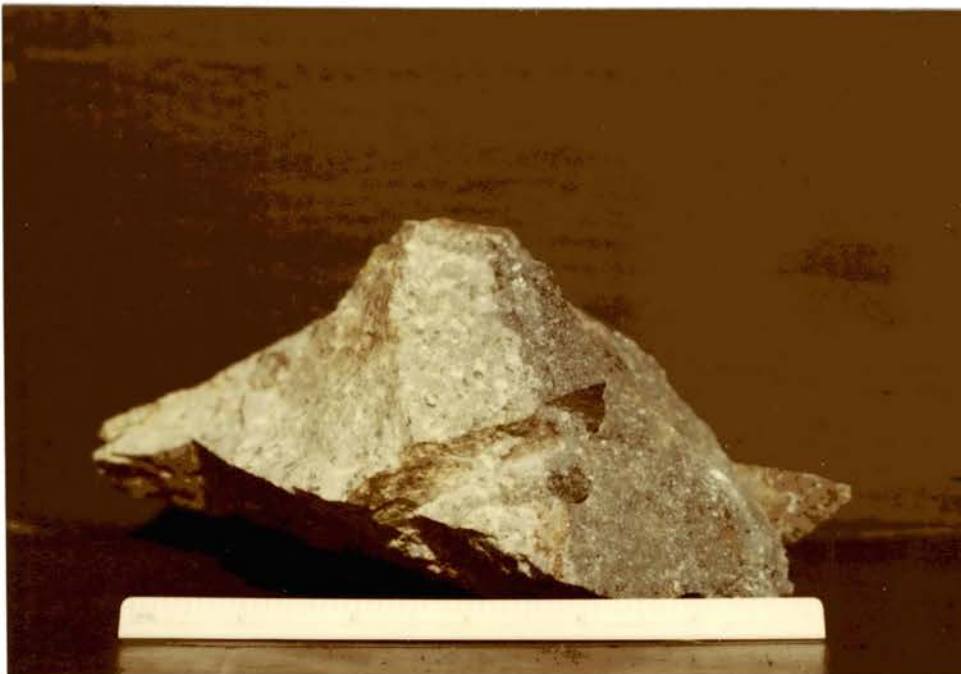


Figure 11. Photograph showing sharp contact and poorly defined chilled margins of quartz latite porphyry dike (left) intruding ash-flow tuff (right).

Quartz phenocrysts are present as euhedral to subhedral crystals ranging from 2mm to 6mm and averaging 4mm in the longest dimension. Some of the crystals are bipyramidal, appearing as squares when broken along their C-crystallographic axes. Crystals are usually fractured, moderately corroded, and embayed (Fig. 12). Quartz displays an absence of

TABLE II
MODAL ANALYSES OF QUARTZ LATITE PORPHYRY DIKES

Constituents	Sample 55	Sample 17
quartz	10.71	10.05
potassium feldspar	7.22	7.13
plagioclase	14.28	14.75
biotite	3.47	2.98
magnetite ¹	2.27	2.22
groundmass	62.03	62.83
Total %	99.98	99.96

¹Includes sphene and apatite.

undulatory extinction and alteration.

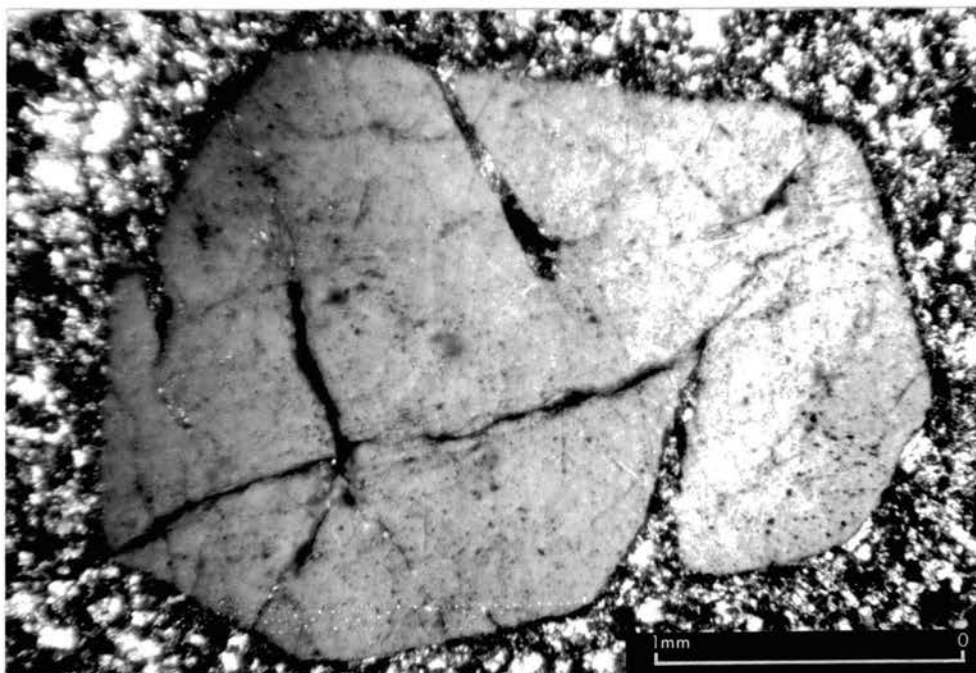


Figure 12. Photomicrograph of corroded and embayed euhedral quartz phenocryst set in a microcrystalline groundmass of quartz, feldspar, and opaques; sample taken from a quartz latite porphyry dike (crossed nicols).

Potassium feldspar phenocrysts occur as euhedral to subhedral crystals ranging from 2mm to 5mm in length and averaging 3mm. Crystals are typically twinned according to the Carlsbad law, exhibit a cloudy appearance, and produce 2V measurements (30 to 35 degrees) indicative of a disordered orthoclase. Several of the phenocrysts poikilolitically enclose unaltered euhedral plagioclase laths ranging up to 1mm in length.

Plagioclase is present in two forms: 1) as euhedral to subhedral laths ranging from 2mm to 4mm in length and averaging 3mm; 2) as clusters

of euhedral to subhedral crystals which as a whole range up to 7mm in the longest dimension. Optical measurements of Carlsbad-albite twinning indicate compositions range from oligoclase (An_{28}) to andesine (An_{32}). Several crystals exhibit oscillatory zonation with intense sericitization of more calcic zones. All crystals exhibit the effects of weak sericitization along fractures and crystal margins. Occasionally, small crystals of biotite, magnetite, and sphene are encased in the plagioclase phenocrysts.

Brown biotite occurs as corroded euhedral to subhedral crystals ranging from 0.5mm to 4mm in length and averaging 1.5mm (Fig. 13). Biotite is typically unaltered, although occasionally it displays chloritization and/or sericitization along cleavage planes and crystal faces. Reaction rims of magnetite are common, usually extending inward along cleavage planes. Magnetite is also present as subhedral to anhedral grains, either within biotite or disseminated through the groundmass. Sphene, which is almost always associated with magnetite and biotite, occurs as euhedral to anhedral crystals that average 0.1mm in length.

The matrix is microcrystalline-equigranular, consisting of indeterminate amounts of quartz, feldspar, and opaques. The grain size approximates 0.03mm although occasionally it is slightly coarser.

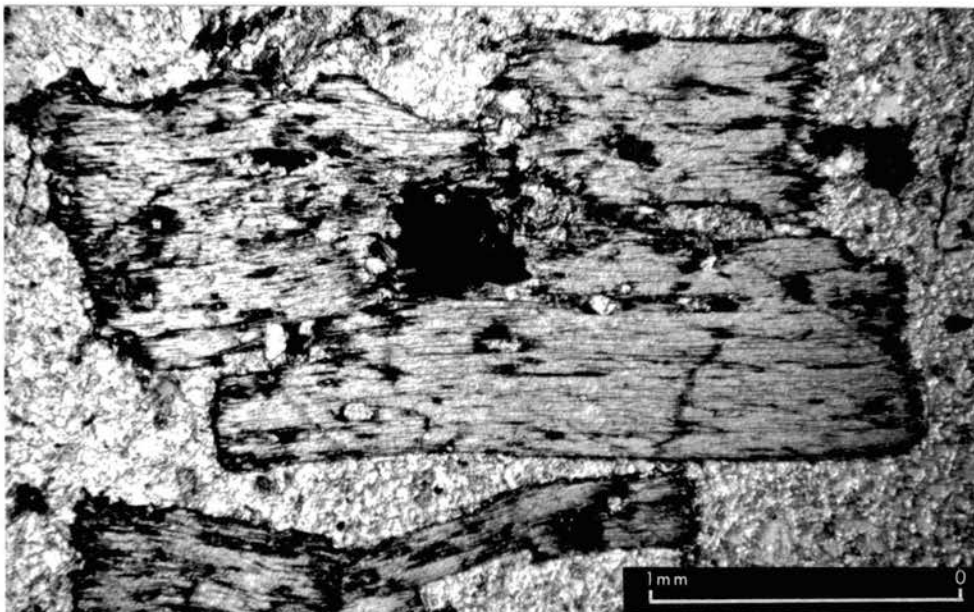


Figure 13. Photomicrograph of embayed brown biotite plates enclosing grains of magnetite and sphene. Note replacement by magnetite along cleavage planes in biotite crystal at lower left hand corner (ordinary light).

Intrusive Breccia Dikes

This term is used to describe breccias emplaced into overlying rock as a result of magmatic (intrusive-explosive) events of a shallow origin. Other names in common use include "pebble dikes" or "igneo-fragmental dikes" (Wallace and others, 1968; MacKenzie, 1970).

Three intrusive breccia dikes are revealed within the quartz latite porphyry stock; others probably exist. The dikes range from one to two feet wide, display sharp contacts, and show pronounced lineation paralleling the wall rock. Outcrops are difficult to distinguish because of ubiquitous limonitic staining and lack of erosional resistance.

When broken, the rock displays angular to subangular fragments of

quartz latite porphyry and quartz set in an intensely silicified pinkish gray aphanitic matrix (Fig. 14). Fragments vary considerably in size ranging from minute grains to pebbles in excess of 3cm in diameter. Careful inspection reveals a plethora of small vugs.



Figure 14. Photograph showing fragmental characteristics of the intrusive breccia dikes.

Thin section studies indicate the rock fragments are mineralogically and texturally equivalent to samples from the intensely altered zones of the quartz latite porphyry stock. Sericitization in these fragments is so extensive that all traces of feldspar and biotite are destroyed. Pyrite, sphene, and rutile are apparent in many fragments.

Dacite Porphyry Dikes

A dacite porphyry dike trending approximately N60W cuts the quartz latite porphyry stock and stockwork mineralization therein. Exposures of the dike exhibit a more or less linear trace extending from the ridge line of Red Mountain into both Lincoln and Peek-a-boo Gulches. Equivalent surface coloration to the country rock and lack of erosional resistance prohibit distinction of the dike on aerial photographs.

The dacite displays phenocrysts of plagioclase, quartz, and "book" biotite set in a greenish-gray aphanitic groundmass. Veinlets and lobate masses of magnetite permeate the rock, distinguishing it from any other in the Red Mountain area (Fig. 15). Petrographic studies indicate that between 15 and 30 percent of the rock is deuteric magnetite with the remainder consisting of a microcrystalline matrix and phenocrysts in the following "approximate" proportions: 17 percent plagioclase, 6 percent quartz, and 5 percent biotite. No potassium feldspar was observed.

Plagioclase phenocrysts occur as fractured euhedral to subhedral laths ranging from 0.5mm to 3.5mm in length, averaging 1.5mm. Typical laths display oscillatory zonation with intense sericitization of the more calcic zones (Fig. 16). Interfaces between altered-unaltered zones are invariably accented by hematitic staining. Occasionally, small euhedral crystals of unaltered apatite occur poikilolitically enclosed in the laths.

Quartz phenocrysts are present as anhedral crystals ranging from 0.3 mm to 2mm in the longest dimension, averaging 0.7mm. Crystals are characterized by extreme corrosion, which relict textures indicate extends inward up to 0.2mm. Quartz displays an absence of undulatory extinction or alteration.

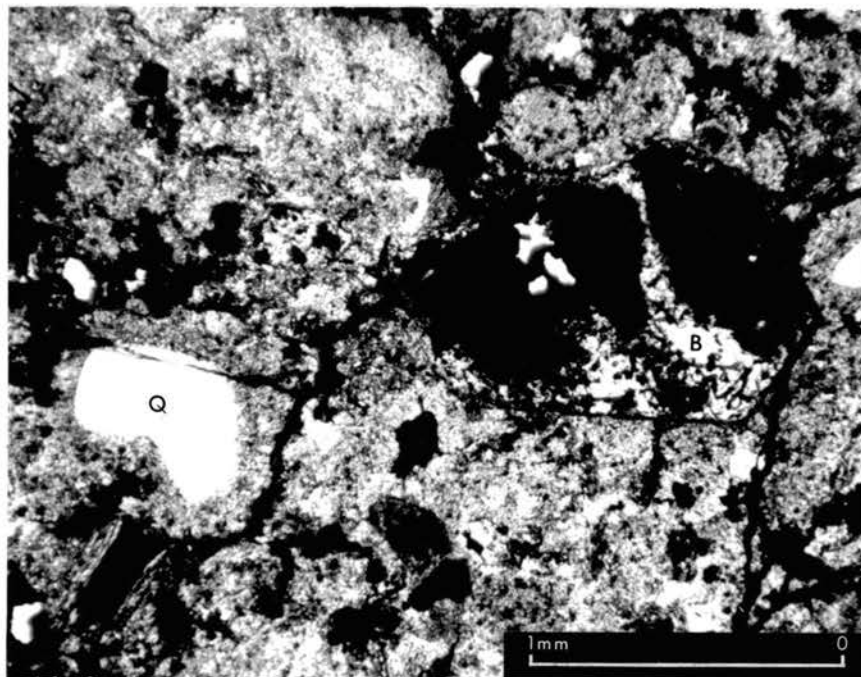


Figure 15. Photomicrograph showing characteristics of dacite porphyry; intensely corroded quartz phenocrysts (Q), biotite plates partially replaced by magnetite (B), veins and lobate masses of magnetite partly altered to hematite. Note hexagonal outline biotite crystal (almost totally replaced by magnetite) in center of photograph (ordinary light).

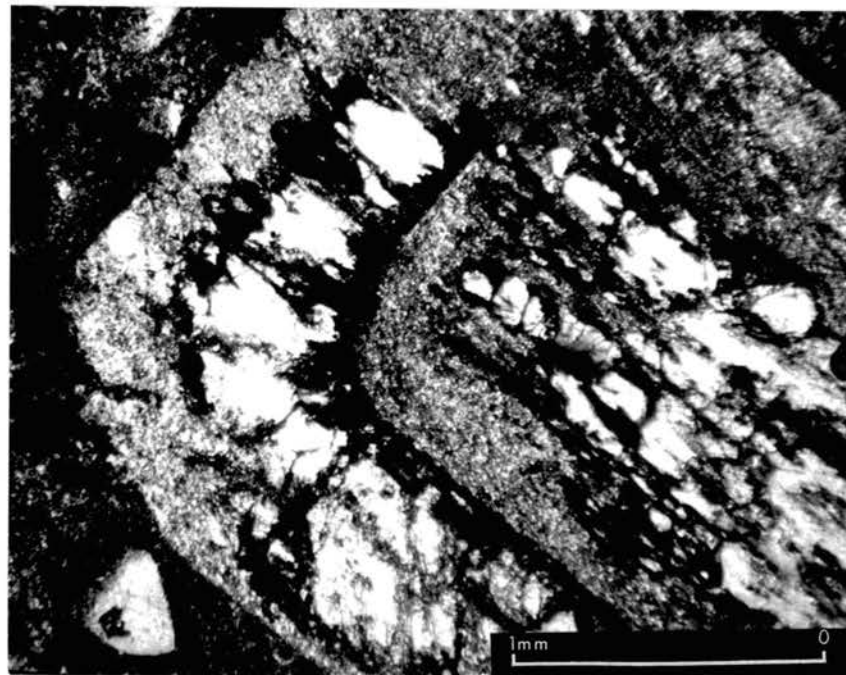


Figure 16. Photomicrograph of plagioclase lath exhibiting oscillatory zonation with intense sericitization of the more calcic zones. Interfaces between altered-unaltered zones are accented by hematitic staining; sample taken from dacite porphyry dike (crossed nicols).

Green biotite occurs as euhedral to subhedral crystals, ranging from 0.5mm to 2mm in the longest dimension, averaging 1mm. Biotite is typically unaltered, although occasionally it displays chloritization and/or sericitization along cleavage planes and crystal margins. Reaction rims of magnetite (partly altered to hematite) are common, usually extending inward along cleavage planes (Fig. 15). Occasionally, almost total replacement of biotite by magnetite is apparent. Minor amounts of euhedral sphene occur encased in the biotite plates.

The matrix of the dacite porphyry is microcrystalline, consisting of partly altered feldspar and minor amounts of quartz. The grain size approximates 0.04mm, although occasionally it is slightly coarser.

Rhyolite Porphyry Dikes

Two rhyolite porphyry dikes are exposed along the ridge line north of the Red Mountain stock, revealing more or less linear traces extending along a N60E trend into Lincoln Gulch. A third dike striking approximately N45E cuts the Red Mountain stock and dacite porphyry dike therein. These rhyolite dikes are 2 to 5 feet wide, display sharp contacts with the country rock, and exhibit pronounced flow banding.

The rhyolite displays small phenocrysts of quartz, feldspar, and biotite set in a silicified-aphanitic groundmass. Petrographic studies indicate 74 percent is matrix with remaining phenocrysts in the following "approximate" proportions: 12 percent quartz, 7 percent potassium feldspar, 5 percent plagioclase, and 2 percent biotite.

Quartz phenocrysts are present as fractured euhedral to subhedral crystals that range from 0.5mm to 3mm in the longest dimension, averaging 1.5mm. Crystals are characterized by moderate corrosion, embayment, and

an absence of undulatory extinction or alteration.

Potassium feldspar and plagioclase phenocrysts occur as fractured euhedral to subhedral crystals that range from 0.5mm to 4mm in the longest dimension, averaging 2mm. Both minerals display the effects of sericitization--plagioclase to a much more intense degree.

Biotite is altered to a mixture of sericite, fine chlorite, and cleavage-controlled grains and lenses of pyrite and leucoxene. These pseudomorphs retain a euhedral form, ranging up to 1.5mm in length.

The groundmass is microcrystalline-equigranular, consisting of quartz and lesser amounts of altered feldspar and opaques. Petrographic studies indicate the grain size approximates 0.02mm.

Precambrian Structure

Foliation and lineation as expressed by parallel orientation of biotite plates, sillimanite prisms, and pegmatitic stringers are well developed in the outcrops of Sawatch Schist and Migmatite in the Red Mountain area. These fabrics are Precambrian in age and regional in character, conforming to the N60E-N80E trend and near vertical dip reported for the metasedimentary rocks of the Independence Pass area (Stark and Barnes, 1935; Tweto and Sims, 1963). From a tectonic standpoint, they are manifestations of a major episode of Precambrian deformation which resulted in high-grade metamorphism and tight isoclinal folding of mica schists along northeast-trending axes (Tweto, 1968).

Tertiary Structure

Igneous Rocks

Figure 3 clearly shows the preferential alignment of porphyry

intrusions along one of two trends. One dike set and the Red Mountain stock strike approximately N20W, paralleling the faults defined along the western flank of Red Mountain. A second set of dikes is well displayed along a N60W trend, aligning with the southwestern ring-fracture zone of the central cauldron block (Candee, 1971). From the regional character of both trends, the author concludes that extensional fractures generated during development of the central cauldron controlled emplacement of the stock, as well as the dikes. Both fracture sets must have been temporally related as evidenced in several cases by N60W-trending offshoots of predominantly N20W-trending quartz latite dikes.

Emplacement of the Red Mountain stock may have proceeded by open space filling, magmatic stoping, forceful injection, or a combination of these mechanisms. Consideration of space requirements coupled with similar attitudes of compactional layering in the ash-flows along either side of the stock indicate magmatic stoping was an important, if not the dominant, emplacement mechanism.

The occurrence of intrusive breccia dikes--as well as the chilled contacts and aphanitic groundmasses which characterize the porphyry stock and dikes--is indicative of a near surface sub-volcanic environment. Although definite proof that a volcano once existed over the present site of Red Mountain is lacking, the indirect evidence is most convincing.

Fractures

A number of N65E-N80E-trending fractures are revealed along prospect pits and short adits in both the quartz biotite monzonite and superjacent ash-flow tuffs (Fig. 3). The fractures range up to eight inches in width, exhibit near vertical dips, and are characterized by gouge,

slickensides, open spaces, and occasionally breccia. They have controlled polymetallic sulfide veins and to the north of the thesis area the emplacement of rhyolite porphyry dikes. This latter association indicates that fracture development postdated emplacement of andesite, quartz latite, and dacite intrusions in the Red Mountain area. The distinctive characteristics of the fractures coupled with their trend--aligning with the southern ring-fracture zone of the central cauldron--is indicative of an extensional development reflecting deformation during later stages of the cauldron cycle. Available evidence indicates the fractures predate the defined faults in the Red Mountain area.

Faults

On the basis of field studies, four major Tertiary faults are distinguished in the thesis area. Two are defined along the western flank of Red Mountain by somewhat arcuate traces (concave to the west) striking approximately N20W. The westernmost of these (Lincoln Gulch fault) extends across the diameter of the Grizzly Peak volcanic field, bisecting the resurgent Lincoln Gulch Stock (Candee, 1971). The other two faults, exhibiting somewhat arcuate traces (concave to the east) striking approximately N35E, are revealed along the eastern flank of Red Mountain. Available evidence indicates all are of a high-angle nature with normal displacement (Fig. 17). No faults were distinguished which could be attributed to a southern ring-fault zone of the central cauldron,

Establishing the absolute age of faults in the thesis area is impossible; however, relative ages can be partially established from the following geologic relationships:

- 1) All of the faults displace the "post-subsidence" slump breccias.

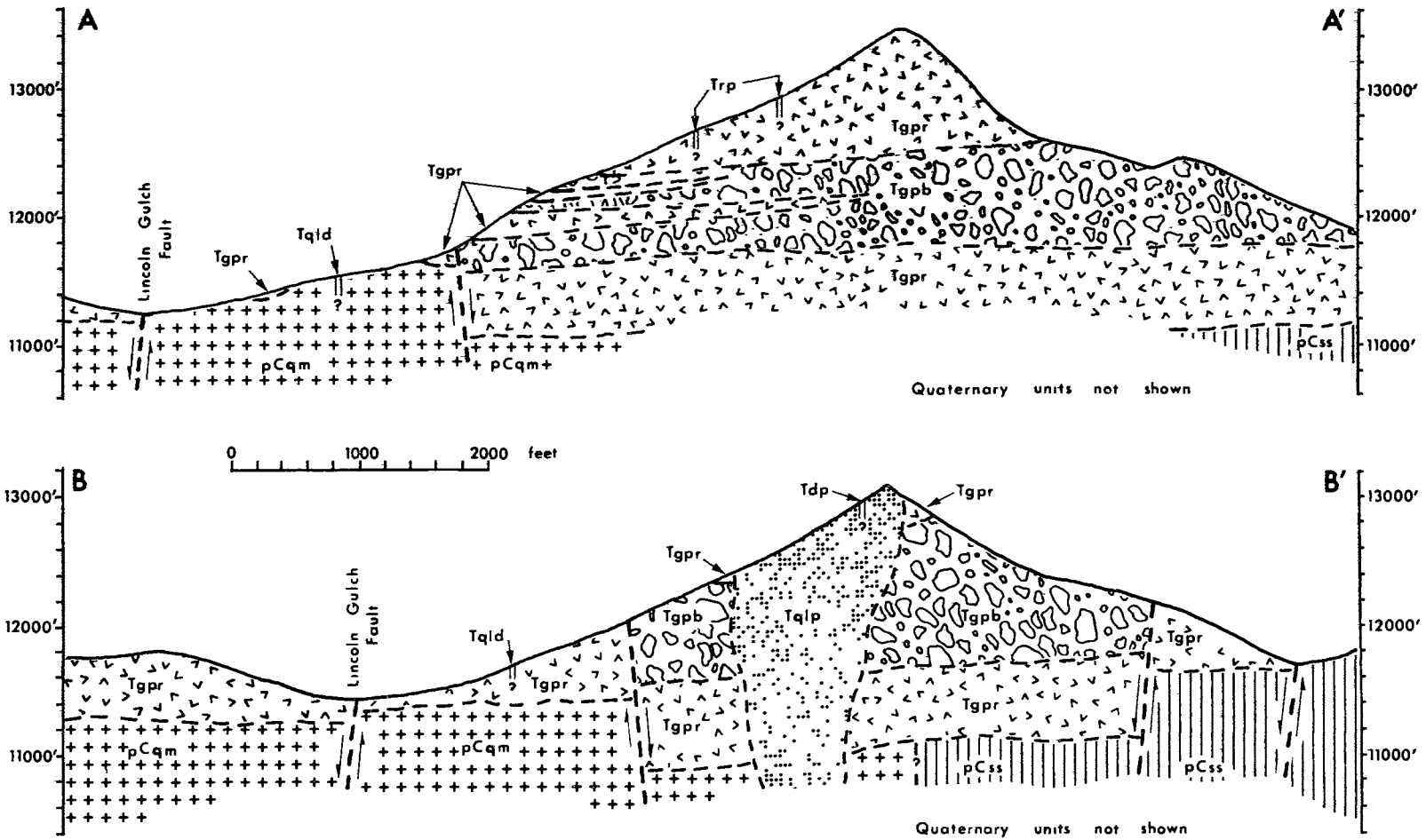


Figure 17. Generalized cross sections through Red Mountain, symbols are as shown on geologic map (Fig. 3).

- 2) The N20W-trending Lincoln Gulch fault displaces the resurgent Lincoln Gulch Stock (Candee, 1971).
- 3) Inspection of adits and prospect pits along faults did not reveal any appreciable hydrothermal alteration and/or metallization, a fact substantiated by trace element studies.
- 4) Intense hydrothermal alteration and coexistent polymetallic mineralization are displayed along N65E-N80E fractures in Lincoln Gulch (see Figure 3 for distribution of fractures relative to faults).

These relationships clearly indicate that development of the faults postdated collapse of the central cauldron block; furthermore, the N20W-trending faults must postdate hydrothermal activity along N65E-N80E fractures. The age relationships presented on page 10 suggest that the N20W-trending faults must also postdate the emplacement of all porphyry intrusions. The four faults, which are thought to be temporally related, may reflect Miocene block faulting (Cruson, oral communication, 1973) or they may manifest "late" adjustments in an underlying magma reservoir. The author prefers the latter explanation since the N20W-trending faults parallel porphyry intrusions.

CHAPTER V

MINERALIZATION

As previously indicated, two major hydrothermal events of mid-Tertiary age are recorded in the Red Mountain area. The first event is evidenced in a quartz-pyrite-molybdenite stockwork permeating the Red Mountain stock. A second and younger event is revealed laterally away from the stock in polymetallic sulfide veins along N65E-N80E-trending fractures. The relative age of these latter veins is clearly evidenced by their spatial association with "late" rhyolite porphyry dikes just north of the thesis area. Crosscutting relationships revealed within the confines of the Red Mountain stock provide evidence that the two hydrothermal events and porphyry intrusions record a cyclic magmatic-hydrothermal history. The author attributes the cyclic history to chemical and physical changes within a single master magma reservoir.

Studies of the younger polymetallic veins were not undertaken and other than the generalized relationships in Figure 18 little of significance may be presented. The remainder of this chapter will deal specifically with the hydrothermal event recorded in stockwork mineralization.

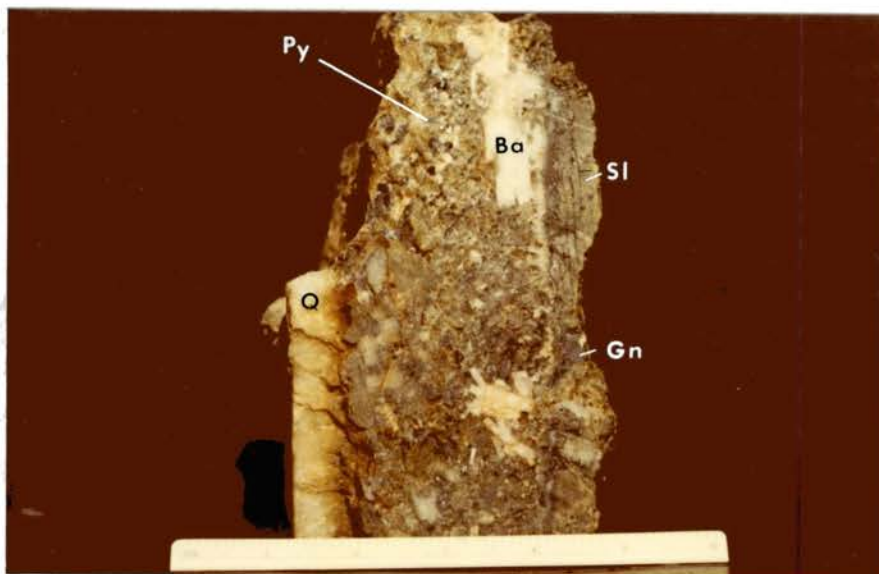


Figure 18. Photograph of an unusually well developed polymetallic vein displaying a more or less symmetrical distribution of comb structure quartz (Q), sphalerite (Sl), and argentiferous (?) galena (Gn). Coarse grains of pyrite (Py), galena, and lesser amounts of chalcopyrite are disseminated through a brecciated and vuggy central core of quartz and sphalerite. Reopening was followed by crystallization of barite (Ba) and lesser amounts of calcite. Sample collected at mine dump north of the thesis area along the eastern flank of Lincoln Gulch. The vein was localized along N70E-trending fracture.

Stockwork Mineralization

Stockwork mineralization is defined in an area approximately equivalent to that enclosed by the inferred configuration of the quartz latite porphyry stock. Mineralization is recorded in three distinct veinlet types (Fig. 19):

- 1) Composite quartz-pyrite-molybdenite veinlets ranging from 0.2mm

to 2mm in width--characterized by random orientation, crosscutting and displacing relationships, matching walls, vugs, comb structure, and crustification--characteristics indicative of open space filling.

- 2) Composite lenticular pods of quartz-pyrite-molybdenite ranging up to 4cm in the longest dimension--characterized by irregular and gradational contacts, islands of wall rock, vugs, comb structure, crustification, and often by type 1 veinlets radiating outward--characteristics, which when coupled with space requirements, are indicative of a combined open space filling and replacement.
- 3) Pyrite veinlets averaging 1mm in width--characterized by random orientation, matching walls, and open spaces--commonly crosscut and displace type 1 and 2 veinlets.

Quartz is by far the most abundant constituent in type 1 and 2 veinlets and in many cases is the only mineral present. It is fine grained, forming a tight interlocking mosaic of anhedral crystals with sutured grain boundaries. Other than minor amounts of vug-filling calcite, quartz was the only gangue mineral encountered.

Pyrite is the dominant metallic mineral in type 1 and 2 veinlets and is the principal constituent of type 3 veinlets. In the veinlet and lenticular pods of quartz, it is typically present as granular masses or clusters of striated cubes, all invariably intergrown with or encrusting drusy vugs. In the type 3 veinlets, pyrite occurs as a more or less continuous chain of striated cubes along fracture surfaces. Most, if not essentially all, of the pyrite in type 1 and 2 veinlets genetically belongs to the later generation of pyrite veinlets.



Figure 19. Photograph displaying a lenticular "pod" shaped quartz vein with thin veinlets of quartz radiating outward. Note island of wall rock within pod, crosscutting and displacing relationship of thin veinlets, and fresh pyrite. Close inspection reveals a thin pyrite veinlet at far left in which pyrite is partly replaced by limonitic minerals.

Limited amounts of molybdenite are revealed in type 1 and 2 composite veinlets--it was not observed in the pyrite veinlets. In the thin quartz veinlets, molybdenite typically is present as small granules or platelets which tend to concentrate in two thin symmetrical bands along vein margins. In the lenticular quartz pods, it occurs as fine grains intergrown with and enclosed by quartz.

Trace Element Study

The primary objectives of this trace element study are to delineate and interpret the distribution of selected "transitional" and

"main-group" metals within and contiguous to the zone of stockwork mineralization. The approach consists of determining "approximation" background values, threshold values, and preparing trace element distribution maps. Correlation coefficients were calculated for values obtained from samples of the stock, as well as all samples collected. Limitations imposed by the methods of sampling and analytical analysis--as well as sample distribution and number of analyses--prohibit an intense statistical treatment of the data.

Methods of Sampling and Analytical Analysis

Bulk hand samples (approximately one pound) were randomly collected from a minimum of two and a maximum of four locations within an outcrop. Each sample was crushed, the freshest-appearing fragments separated and combined with those of the other samples from the outcrop. The composite samples were then analyzed by means of atomic absorption spectrometry for copper, zinc, lead, molybdenum, and tungsten. Skyline Labs, Inc., of Wheat Ridge, Colorado, completed the analytical work. Results of the analyses and index map to sample locations are presented respectively in Appendix B and Figure 20.

Background and Threshold Values

Background values for the rhyolitic ash-flow tuffs may be approximated from the values of 12 unaltered and xenolith free samples representing different stratigraphic horizons. Data descriptions of these 12 selected samples are presented in Table III along with corresponding world averages for granitic rocks (Turekian and Wedepohl, 1961; Vinogradov, 1962). The data clearly reveal that molybdenum and tungsten

TABLE III

DATA DESCRIPTION OF TRACE ELEMENT VALUES FROM SELECTED SAMPLES OF ASH-FLOW TUFF¹

	n	Arithmetic Mean	Std. Dev.	Maximum	Minimum
ASH-FLOW TUFF ^{2,3}					
copper	12	11.66	10.52	40	5
lead	12	18.75	12.81	40	5
zinc	12	67.92	24.91	115	40
molybdenum	12	3.00	1.86	8	2
tungsten	12	2.17	0.39	3	2
WORLD AVERAGES FOR GRANITIC ROCKS ⁴					
		TW	V		
copper		10	20		
lead		19	20		
zinc		39	60		
molybdenum		1.3	1		
tungsten		2.2	1.5		

¹All values in parts per million.

²Samples no. 2, 7, 8, 9, 33, 34, 36, 37, 39, 54, 59, 61--SEE INDEX MAP OF SAMPLE LOCATIONS (Fig. 20).

³Numerical value of (X) was used for statistical treatment where values were reported as "less than" (X) (Appendix B).

⁴Data in column labeled TW are from Turekian and Wedepohl (1961); data in column labeled V are from Vinogradov (1962).

deviate slightly from the arithmetic mean, whereas zinc, copper, and lead exhibit large deviations; furthermore, the mean values are in excellent agreement with world averages. From these considerations, the author concludes the following:

- 1) The arithmetic means for molybdenum and tungsten are a reasonable approximation of the mean average background values for these metals in the rhyolite ash-flow tuffs.
- 2) The quantity of copper, zinc, and lead in any one sample is greatly variable (especially zinc); therefore, the range between maximum and minimum in Table III is a more accurate representation of the background for these elements.

Data descriptions for all rock types (67 samples) and the 16 samples from the Red Mountain stock are presented in Table IV along with corresponding threshold values. These latter values are the end result of plotting frequency diagrams, setting restrictive ranges at the 5 percent level, computing arithmetic means and standard deviations, and adding two times the standard deviation to the mean. From the data, the following significant observations are drawn:

- 1) Threshold values for the composite rock types are a suitable means for determination of anomalous (+) values in the Red Mountain area; however, thresholds for copper, lead, and tungsten seem rather high when compared with the data in Table III.
- 2) Copper and lead threshold values for the Red Mountain stock are less than those thresholds for the total population of samples, a result of smaller standard deviations. The threshold value for zinc is less because of a greatly decreased mean value, as well as a decreased standard deviation.

TABLE IV

DATA DESCRIPTION OF TRACE ELEMENT VALUES FROM ALL ROCK TYPES AND QUARTZ LATITE ROCK¹

	n	Restrictive Range	Arithmetic Mean	Std. Dev.	Threshold ² Value
ALL ROCK TYPES ³					
copper	67	200	28.92	33.10	95.13
lead	67	70	23.93	16.15	56.24
zinc	67	130	48.79	38.35	125.50
molybdenum	67	15	2.94	1.90	6.74
tungsten	67	15	3.66	2.54	8.74
QUARTZ LATITE STOCK ⁴					
copper	16	200	33.75	17.08	67.91
lead	16	70	24.06	12.68	49.41
zinc	16	130	9.06	4.17	17.40
molybdenum	16	15	5.33	5.77	16.88
tungsten	16	15	5.64	1.78	9.20

¹All values in parts per million.

²Calculated by adding 2(Std. Dev.) to the arithmetic mean (Hawkes and Webb, 1962).

³Numerical value of (X) was used for statistical treatment where values were reported as "less than" (X) (Appendix B).

⁴Samples no. 18, 19, 20, 21, 23, 25, 27, 28, 29, 45, 66, 68, 69, 70, 71, 72--SEE INDEX MAP OF SAMPLE LOCATIONS (Fig. 20).

- 3) Molybdenum and tungsten threshold values for the Red Mountain stock are larger than those thresholds for the total population of samples, a result of larger mean values and in the case of molybdenum, a larger standard deviation.

Trace Element Distribution Maps

Trace element distribution maps are presented in Figure 21. Outcrops within and marginal to the stock are displayed. Contouring was done on large intervals to show trends rather than local variations.

The information contained in each map is well displayed and summarized in part as follows:

- 1) Molybdenum, and in general tungsten, are positive anomalies in the stock, the highest values of both metals occur in a N20W-trending elliptical area paralleling the trend of the stock.
- 2) Zinc is clearly a negative anomaly in the stock, the lowest values occurring in an area corresponding more or less to the N20W-trending zone of high molybdenum.
- 3) Lead and copper are neither positive or negative anomalies in the stock; however, the lowest values of both are present in an area roughly analogous to the zone of high molybdenum.
- 4) There is an apparent absence of any primary halo within the ash-flow tuffs enveloping the stock and stockwork mineralization therein.¹

¹The reader should observe the alteration map (Fig. 21).

Correlation Coefficients

Correlation coefficients were calculated for the 16 samples of the Red Mountain stock and total of 67 samples from the Red Mountain area. The correlation matrices in Table V display the results.

At a 5 percent significance level, a meaningful correlation for the 16 quartz latite samples and five variables (copper, zinc, lead, molybdenum, and tungsten) is 0.67 (Neville and Kennedy, 1964). On this basis, only the correlation between molybdenum and tungsten is significant. When coupled with previous considerations of trace element distribution, this correlation provides evidence that molybdenum and tungsten were concentrated both contemporaneously and spatially.

For the total 67 samples and five variables, a meaningful correlation at the 5 percent significance level is 0.36. Inspection of Table V reveals significant correlations for molybdenum-tungsten and lead-zinc. These correlations are probably manifestations of the two hydrothermal events, but they may also in part reflect orthomagmatic relationships.

Discussion of Stockwork Mineralization

The spatial restriction of stockwork mineralization to the Red Mountain stock is well displayed and clearly reveals a genetic association. Similar cases, in which a stockwork is confined to a Tertiary intrusive complex, are well documented in the Colorado mineral belt. Most notable of these are the Henderson and Climax molybdenite deposits, the former most ably described by MacKenzie (1970), the latter by Wallace and others (1968). Parts of the ensuing discussion are based on the concept of these authors.

The author speculates stockwork fractures formed as a result of

TABLE V
CORRELATION COEFFICIENT MATRICES FOR TRACE ELEMENT VALUES

ALL SAMPLES (n=67)					RED MOUNTAIN STOCK (n=16)				
Cu	Pb	Zn	Mo	W	Cu	Pb	Zn	Mo	W
Cu	-0.04	0.03	0.00	-0.02	Cu	0.00	0.00	0.04	0.01
Pb		0.76	0.21	-0.19	Pb		0.00	-0.01	-0.03
Zn			0.01	-0.04	Zn			0.01	0.00
Mo				0.89	Mo				0.75
W					W				

multiple magmatic and/or hydrothermal adjustments in a magma column underlying congealed levels of the Red Mountain stock. A N20W-trending "main" fracture system, which controlled the introduction(s) of hydrothermal fluids, is thought to be evidenced by the elliptical area of high molybdenum values. Support for this interpretation is gained by considering the structural controls of stock emplacement (see page 36).

The end result of hydrothermal activity is evidenced in the myriad of quartz-molybdenite veinlets. These veins, which formed both by replacement and open space filling, consist primarily of quartz with minor amounts of molybdenite concentrated along veinlet margins. Trace element studies provide evidence that molybdenite was accompanied by a temporal and spatial enrichment of tungsten, probably as one of the wolframite group minerals. No tungsten-minerals were identified in the present study.

The major introduction of pyrite clearly postdated emplacement of the quartz-molybdenite veins. This relationship may reflect a younger and separate introduction of hydrothermal fluid or may be due to overlap by simultaneously retreating fronts of contemporary quartz-molybdenite and pyrite deposition during the waning stage of hydrothermal activity. The author prefers the first explanation.

Trace element studies indicate that lead and copper are neither positive or negative anomalies in the stock; however, the lowest values of both are present in an area roughly analogous to the N20W-trending zone of high molybdenum values. Previous considerations clearly reveal that zinc is anomalously low in the stock, particularly along the zone of high molybdenum. These relationships could reflect the increased mobility of zinc relative to copper and lead in the supergene environment

(Hawkes, 1957). The zonal distribution of these metals, however, when coupled with the abundance of fresh pyrite do not support this mechanism. The author concludes the mechanism must have been hydrothermal, the zonal distributions recording mobility away from the N20W-trending main fracture system. From this supposition, zinc would, by necessity, have been more mobil than either lead or copper at some time during the hydrothermal event.

Ash-flow tuffs contiguous to the stockwork were apparently impermeable to fluid transfer, manifestations of the intense compactional welding and method of stock emplacement. Evaluation of metallization in the slump breccias, which undoubtedly were permeable to hydrothermal fluids, was not undertaken in the present study,

CHAPTER VI

ALTERATION

The most conspicuous feature of Red Mountain is, as the name implies, its surface coloration. These yellowish orange to reddish brown colors (see Fig. 22), a visible manifestation of supergene alteration, set Red Mountain apart from neighboring peaks and are in themselves indicators of previous hydrothermal activity.

Three periods of hydrothermal alteration are recorded in the surface rocks of the Red Mountain area. The two earlier periods are related temporally and spatially to the quartz-pyrite-molybdenite stockwork and polymetallic sulfide veins. These two periods are in all probability genetically related to the crystallization of a single master magma reservoir. A third and much later period of hydrothermal alteration is revealed along the N20W and N35E-trending faults. This alteration is very weakly defined and did not accompany any appreciable metallization.

Alteration of a deuteric origin is apparent in those Tertiary rocks which have not undergone extensive hydrothermal alteration. In the ash-flow tuffs and quartz latite dikes, it is typified in weak sericitization and/or chloritization of biotite and sericitization of feldspar. The large amount of magnetite in the dacite dike--revealed in fracture controlled veins and replacing most orthomagmatic minerals--is likewise attributed to a deuteric origin.



Figure 22. Red Mountain looking south along the Continental Divide.

Hydrothermal Alteration Associated With Stockwork Mineralization

Hydrothermal alteration related directly to the N20W-trending stockwork is recorded in four distinct and somewhat systematic zones (Fig. 21). These zones, starting with the more intense alteration type, are as follows:

- 1) Silicified zone.
- 2) Sericitic zone.
- 3) Intermediate argillic zone.
- 4) Less-intense argillic zone.

The zonal classification used here corresponds in general to that proposed by Meyer and Hemley (1967). Use of the term "less-intense argillic" is justified on the basis of decreased alteration intensity with slight mineralogical differences from intermediate argillic alteration. The less-intense argillic alteration locally grades into propylitic alteration; however, the occurrence and intensity of this latter alteration type are so restricted, that they do not warrant special consideration.

Alteration in both the silicified and sericitic zones corresponds to the quartz-sericite-pyrite alteration facies of Creasy (1966). The intermediate and less-intense argillic zones (except for the local areas of propylitic alteration) would be grouped under Creasy's classification as an argillic alteration facies.

Procedure

Samples for study were randomly collected from surface outcrops of the Red Mountain stock and surrounding ash-flow tuffs. Bulk rock samples from the various alteration zones were slabbed and corresponding thin

sections prepared. Altered feldspar phenocrysts were hand-separated from approximately 20 of the rock slabs. The separates were pulverized in a mortar, mounted on porcelain plates, and continuously scanned in a General Electric X-ray diffractometer at a speed of two degrees per minute. Cu K_α radiation was used with an operating voltage of 40kv and 20ma at a sensitivity of 500 cps.

In addition to the altered feldspar phenocrysts, X-ray diffraction analyses were completed for the various limonitic coatings which provide the surface coloration at Red Mountain.

Sericitic Zone

This alteration zone is dominant within the Red Mountain stock, and therefore, most closely associated with the plethora of veinlets that make up the stockwork. Alteration has resulted in a total rock replacement by masses of coarse sericite intermixed with anhedral grains of quartz and lesser amounts of finely disseminated pyrite. Occasionally, remnants of polysynthetic twinning are recorded in thin lenses of coarse sericite arranged in a closely spaced fashion (Fig. 23). Other than these relicts, all traces of any orthomagmatic feldspar have been destroyed. Former biotite sites are clearly evidenced by a variable mixture of rutile, pyrite, and muscovite (Fig. 24). Rutile and pyrite grains noticeably display an absence of preferred orientation and/or alignment.

Silicified Zone

Sericitic alteration grades locally into zones of finely crystalline white to light gray hydrothermal quartz with lesser amounts of sericite,

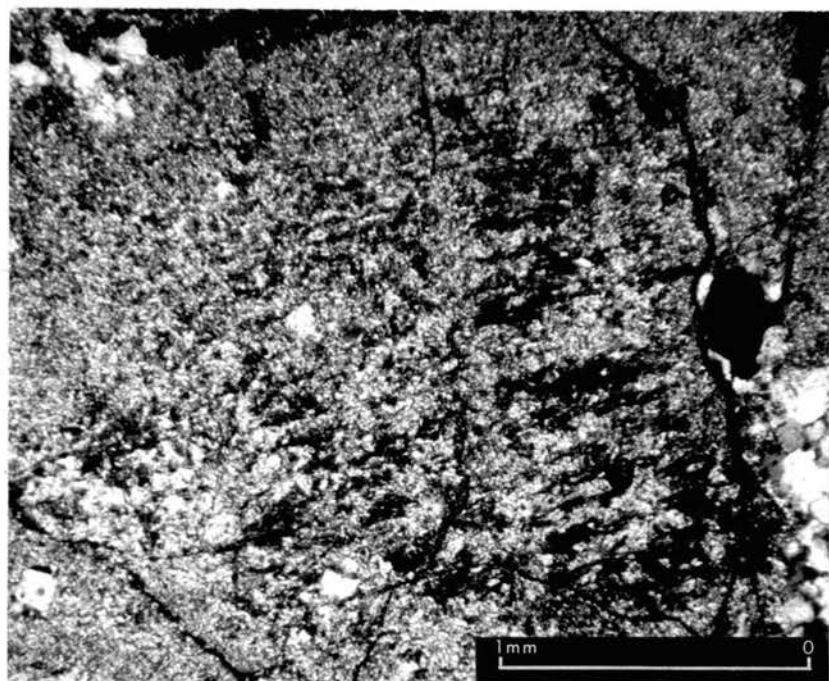


Figure 23. Photomicrograph showing an intensely sericitized plagioclase phenocryst in which ghosts of polysynthetic twinning are recorded. Dark areas within phenocryst are predominately jarosite. Sample was collected from an outcrop within the sericitic alteration zone of the Red Mountain stock (crossed nicols).

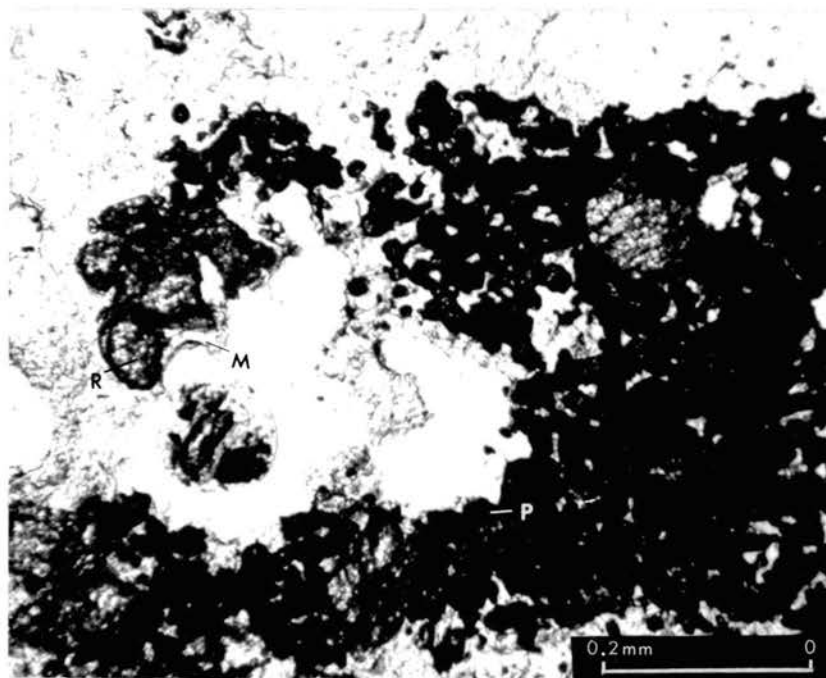


Figure 24. Photomicrograph showing a mixture of rutile (R), pyrite (P), and muscovite (M) arranged after orthomagmatic biotite. Sample taken from an outcrop within the sericitic alteration zone of the Red Mountain stock (ordinary light).

pyrite, and rutile. These leucocratic rocks are prominent in two areas, one within the stock, the other beyond the eastern margin of the stock. Within these zones, replacement by silica has been so complete that only a few scattered remnants of the original rock have escaped destruction. Most of these, although they can be recognized as relicts of earlier rocks, cannot be specifically identified.

Silicification east of the stock grades outward into intense silica cementing, which binds the igneous and metamorphic fragments of the slump breccias. Alteration of the fragments themselves is minor and recorded in the partial destruction of plagioclase and biotite. The slump breccias west of the stock show the same characteristics.

Intermediate Argillic Zone

The sericitic zone grades outward into a thin and somewhat discontinuous envelope of intermediate argillic alteration. This alteration, although pervasive, has not resulted in the textural destruction evidenced in the sericitic zone. Plagioclase is totally replaced by a mixture of fine sericite and montmorillonite (Fig. 25). K-feldspar is relatively fresh, altered to sericite along crystal margins and fractures. Biotite is altered to a muscovite pseudomorph enclosing cleavage-oriented grains and lenses of pyrite and rutile (Fig. 26).

Less-Intense Argillic Zone

The sericitic and intermediate argillic zones grade outward into a wide envelope of less-intense argillic alteration visibly apparent in hydrothermal bleaching (Fig. 27). This alteration, which locally grades into a propylitic alteration type, extends outward in the ash-flows for

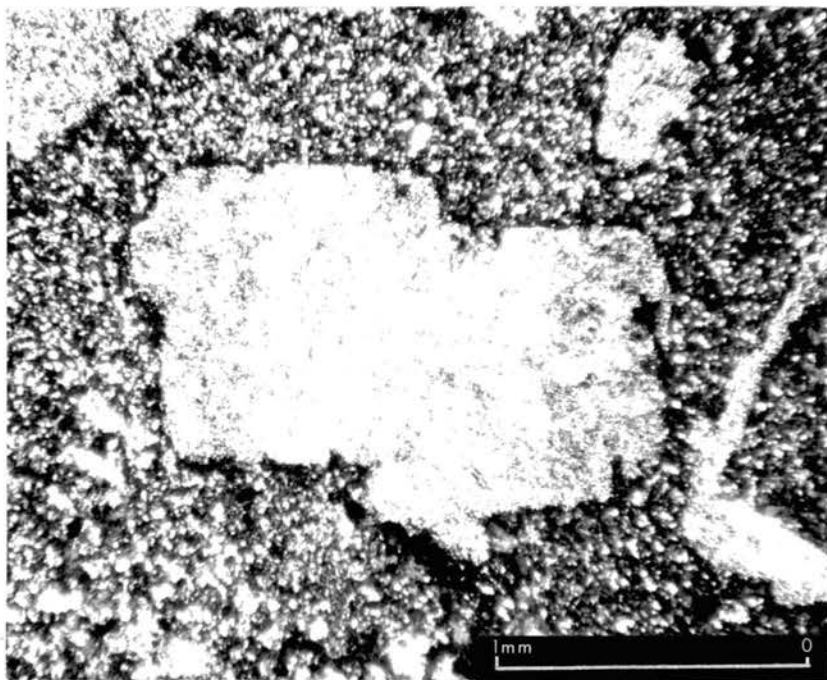


Figure 25. Photomicrograph of a plagioclase lath altered to fine sericite and montmorillonite. Sample taken from an outcrop within the intermediate argillic alteration zone of the Red Mountain stock (ordinary light).

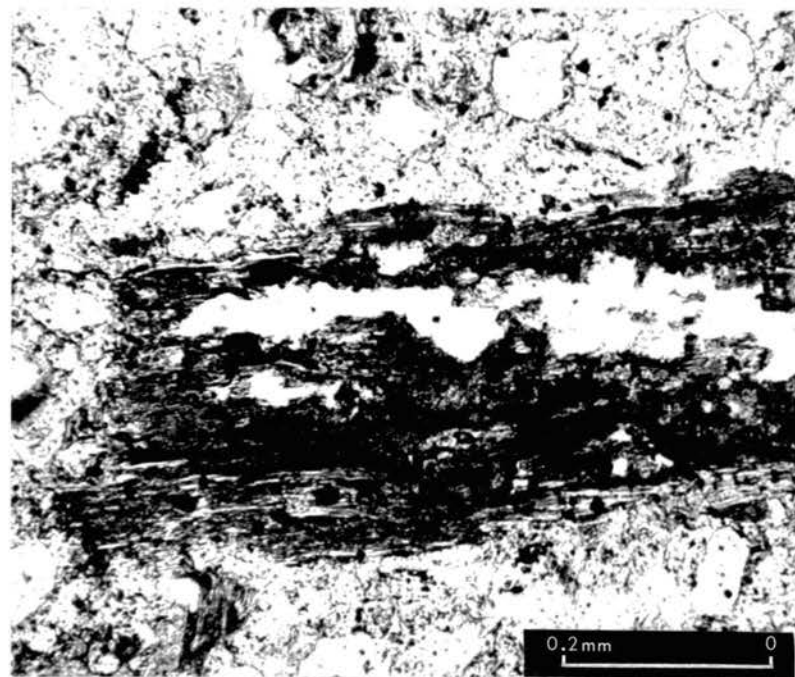


Figure 26. Photomicrograph of a biotite crystal altered to muscovite and cleavage-oriented grains and lenses of pyrite and rutile. Sample collected from an outcrop within the intermediate argillic alteration zone of the Red Mountain stock (ordinary light).



Figure 27. Photograph showing the progressive degree of hydrothermal bleaching toward the Red Mountain stock. All samples are ash-flow tuff.

approximately 500 feet. Plagioclase is replaced by clay, which X-ray diffraction patterns reveal is predominantly montmorillonite (Fig. 28). In the more intensely bleached rock, these clays are diluted with finely disseminated sericite. In the areas of propylitic alteration, the montmorillonite occurs with calcite and epidote, with or without sericite. Biotite is altered to a mixture of sericite, very fine chlorite, pyrite, and leucoxene (Fig. 29). These latter two minerals occur as grains and lenses along cleavage planes and crystal margins. K-feldspar is fresh except in the most intensely bleached rocks where it is sericitized along margins and fractures.

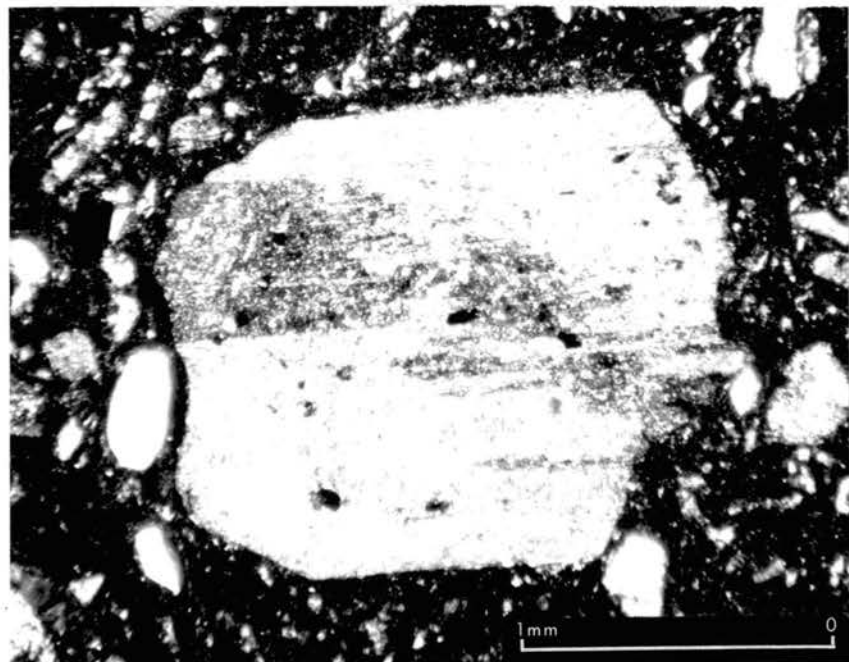


Figure 28. Photomicrograph of a plagioclase crystal weakly altered to montmorillonite and finely disseminated sericite. Sample collected from an outcrop within the less-intense argillic alteration zone of the ash-flow tuff (crossed nicols).

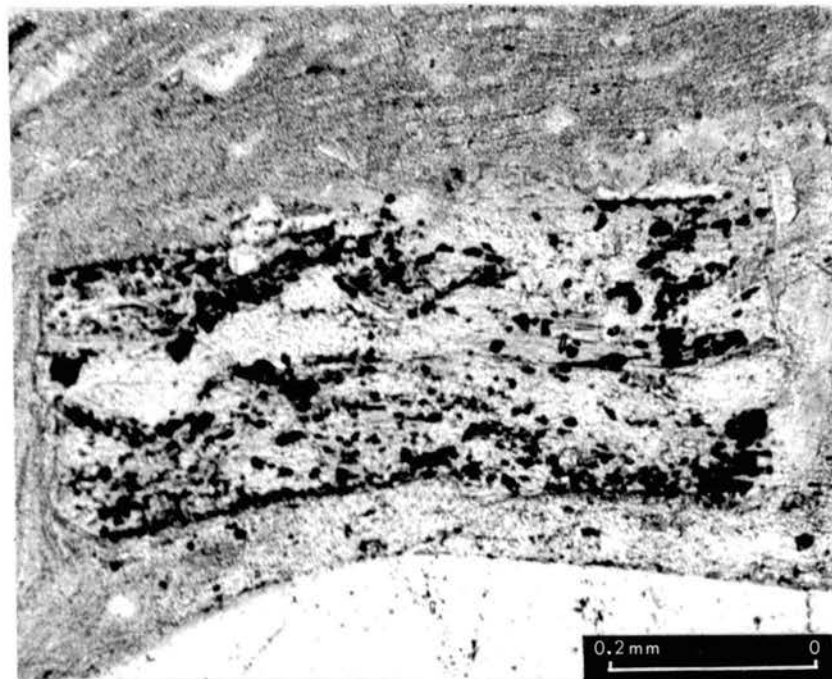


Figure 29. Photomicrograph of a biotite crystal partly altered to sericite, fine chlorite, and cleavage-oriented grains and lenses of pyrite and brown leucoxene. Sample taken from an outcrop within the less-intense argillic alteration zone of the ash-flow tuff (ordinary light).

Discussion

Hydrothermal alteration within and contiguous to the Red Mountain stock is obviously related to the myriad of veinlets that make up the stockwork. The author speculates that alteration and mineralization occurred simultaneously, both resulting from the introduction(s) of hydrothermal fluid. The fluids are presumed to have been aqueous and derived in large, if not entirely, from a crystallizing magma underlying the Red Mountain stock.

The zones of pervasive alteration reflect the passage of at least two chemically different hydrothermal solutions (see page 51). Because of the zonal distribution, however, the author believes most of the alteration, with possible exception of the silicification east of the stock, resulted from a single major introduction of hydrothermal fluid corresponding in age to the quartz-molybdenite veins. The chemical composition of the fluid may have changed primarily through reaction with wall rock, the resultant alteration zones representing the outward variation in temperature, pressure, and chemistry.

According to the concepts of hydrogen metasomatism (Hemley and Jones, 1964), the progressively less intense alteration of feldspar--sericitic zone → less-intense argillic zone--records an increasing base cation/ H^+ ratio in the altering fluids as they migrated outward. It seems unlikely that there was sufficient K^+ released through the sericitization of K-feldspar in the sericitic zone to account for the amount of sericite in the intermediate and less-intense argillic zones (Appendix A, note increased percentages of K_2O in quartz latite stock relative to unaltered quartz latite dikes). Potassium, therefore, must have been in part hydrothermally introduced. The K^+/H^+ ratio and/or

temperature was sufficient to prohibit either the formation of secondary K-feldspar or kaolinite.

An upper temperature limit for montmorillonite in the intermediate argillic zone can be set at 450°C (Hemley and Jones, 1964). Sericite decomposes at approximately 600°C, therefore, setting an upper temperature limit for the sericitic zone.

Supergene Alteration

Supergene alteration, although markedly displayed in surface colors, is not strongly developed in the Red Mountain area. The topographic relief, recent glaciation, dry cool climate, and geologic youth have restricted chemical weathering to the very near surface environment. Evidence of this is well displayed by the abundance of unaltered pyrite in freshly broken rock from the sericitic alteration zone.

The yellowish orange to reddish brown alteration colors distributed over Red Mountain appear intensified because they are superimposed upon hydrothermally bleached rock. Except for the darker shades, which are somewhat more common along intermittent streams and adjacent to the stock, the colors appear randomly distributed and variable in the degree of their intensity.

All colors are due to a soft but compact surface and fracture coating that easily rubs off on hands and clothing. X-ray diffraction patterns of these coatings reveal they consist of pale yellow jarosite ($K_2O \cdot 3Fe_2O_3 \cdot 4SO_3 \cdot 6H_2O$) with sufficient amounts of reddish brown goethite ($Fe_2O_3 \cdot H_2O$) to provide the various colors (Fig. 30). No reflections for hematite were seen in any of the X-ray diffraction patterns.



Figure 30. Photograph showing typical surface colors expressed at Red Mountain. X-ray diffraction patterns reveal the yellowish orange coatings to consist of pale yellow jarosite (far left) with sufficient amounts of reddish brown goethite (far right) to provide the respective color.

From the above considerations, it is evident that jarosite accumulated where sufficient iron and sulfur were available from pyrite and where potassium was available from sericite or K-feldspar. Goethite was undoubtedly precipitated from solution; however, studies of jarosite-goethite equilibrium (Blanchard, 1968) in an environment like that at Red Mountain, provide evidence that goethite may have formed in part as the weathering product of jarosite. Support of this latter consideration is given by the apparent concentration of goethite along intermittent streams within the confines of the stock. A review of the literature indicates pyrite (or total sulfide) content was at least 5 percent within the stock as evidenced by the presence of jarosite. Moving laterally

into the ash-flows, pyrite was appreciably less abundant, thus favoring the formation of goethite.

Thin deposits of reddish brown ferricrete are revealed along the lower elevations of Red Mountain where descending meteoric waters lose velocity. These accumulations of "rust" are characterized by an earthy to somewhat cellular structure and numerous "accidental" fragments of ash-flow tuff. X-ray diffraction and rapid chemical analyses indicate they are isomorphous, consisting primarily of iron and water with minor amounts of the less-soluble salts. With sufficient time, these freshly precipitated ferric hydroxides will convert to the more stable crystalline form of goethite (Garrels and Christ, 1965).

CHAPTER VII

SUMMARY

Relief in the Red Mountain area provides a composite 1,800 foot vertical section of interstratified ash-flow tuffs and slump breccias unconformably overlying a Precambrian basement of metasedimentary and igneous rocks. These country rocks are intruded by a quartz latite porphyry stock (referred to as the Red Mountain stock), intrusive breccias, and porphyry dikes of andesite, dacite, rhyolite, and quartz latite composition. A partial sequence as expressed by crosscutting relationships of the surface Tertiary rocks can be summarized as follows:

youngest - (5) rhyolite porphyry dikes (Trp)

(4) dacite porphyry dikes (Tdp)

(3) intrusive breccia dikes (Tib)

(2) quartz latite porphyry stock (Tqlp) ← ? → quartz latite porphyry dikes (Tqld)

← ? → andesite porphyry dikes (Tap)

oldest - (1) crystal-rich rhyolitic ash-flow tuffs (Tgpr) and interbedded slump breccias (Tgpb).

Studies clearly reveal preferential alignment of porphyry intrusions along N20W and N60W trends. From the regional character of both trends,

the author concludes:

- 1) Red Mountain is within a poorly defined southern ring-fracture zone of the central cauldron block.
- 2) Extensional fractures generated during development of the central cauldron controlled emplacement of the stock as well as the dikes.

Consideration of space requirements coupled with a probable lack of country rock plasticity and similar attitudes of compactional layering in the ash-flows supports magmatic stoping as the dominant mechanism for emplacement of the Red Mountain stock. The occurrence of intrusive breccia dikes--as well as the chilled contacts and aphanitic groundmasses which characterize the porphyry stock and dikes--is indicative of a near surface sub-volcanic environment. Although definite proof that a volcano once existed over the present site of Red Mountain is lacking, the indirect evidence is most convincing.

A number of N65E-N80E-trending fractures are revealed in both the quartz biotite monzonite and superjacent ash-flow tuffs. The fractures, which are characterized by gouge, slickensides, open spaces, and occasionally breccia, have controlled the emplacement of rhyolite dikes just north of the thesis area. This latter association indicates that fracture development postdated emplacement of andesite, quartz latite, and dacite intrusions in the Red Mountain area. The characteristics of the fractures coupled with their trend--aligning with the southern ring-fracture zone of the central cauldron--is indicative of an extensional development reflecting deformation during later stages of the cauldron cycle.

On the basis of field studies, four major Tertiary faults are

distinguished in the thesis area. Available evidence indicates all are of a high-angle nature with normal displacement. Geologic relationships clearly show that development of the faults postdated collapse of the central cauldron block, emplacement of the porphyry stock and dikes, and development of the fractures. The four faults may reflect Miocene block faulting or they may manifest "late" adjustments in an underlying magma reservoir. The author prefers the latter explanation. No faults were distinguished which could be attributed to a southern ring-fault zone of the central cauldron.

A major hydrothermal event is recorded in a quartz-pyrite-molybdenite stockwork permeating the Red Mountain stock. The author speculates stockwork fractures formed as a result of multiple magmatic and/or hydrothermal adjustments in a magma column underlying congealed levels of the stock. A N20W-trending "main" fracture system, which controlled the introduction(s) of hydrothermal fluids, is thought to be revealed by the elliptical area of high molybdenum values.

The end result of hydrothermal activity is evidenced in the myriad of quartz-molybdenite veinlets. These veins, which formed both by replacement and open space filling, consist primarily of quartz with minor amounts of molybdenite concentrated along veinlet margins. Trace element studies provide evidence that molybdenite was accompanied by a temporal and spatial enrichment of tungsten, probably as one of the wolframite group minerals. The major introduction of pyrite clearly postdated emplacement of the quartz-molybdenite veins. This relationship may reflect a younger and separate introduction of hydrothermal fluid or may be due to overlap by simultaneously retreating fronts of contemporary quartz-molybdenite and pyrite deposition during the waning stage of hydrothermal

activity. The author prefers the first explanation.

Ash-flow tuffs marginal to the stock were apparently impermeable to fluid transfer, manifestations of the intense compactional welding and method of stock emplacement.

A second and younger hydrothermal event is recorded laterally away from the stockwork in polymetallic sulfide veins along N65E-N80E-trending fractures. The relative age of these veins is clearly shown by their spatial association with "late" rhyolite porphyry dikes just north of the thesis area.

Crosscutting relationships revealed within the confines of the Red Mountain stock

youngest - (4) rhyolite porphyry dikes (Trp) ? polymetallic sulfide
 ↑
 ↓ mineralization

(3) dacite porphyry dikes (Tdp)

(2) stockwork mineralization

oldest - (1) quartz latite porphyry stock (Tqlp)

provide evidence that the two hydrothermal events and porphyry intrusions record a cyclic magmatic-hydrothermal history. The author attributes the cyclic history to chemical and physical changes within a single master magma reservoir.

Hydrothermal alteration directly relatable to the N20W-trending stockwork is recorded in four distinct and somewhat systematic zones: silicified zone, sericitic zone, intermediate argillic zone, and less-intense argillic zone. The less-intense argillic alteration locally grades into propylitic alteration; however, the occurrence and intensity of this latter alteration type are very restricted. On the basis of

distribution, the author believes most, if not essentially all, of the alteration resulted from a single major introduction of hydrothermal fluid corresponding in age to the quartz-molybdenite veins. The chemical composition of the fluid may have changed primarily through reaction with wall rock, the resultant alteration zones representing the outward variation in temperature, pressure, and chemistry.

Supergene alteration, although markedly displayed in surface colors, is not strongly developed in the Red Mountain area. All colors are due to soft but compact surface coatings which X-ray diffraction patterns reveal are mixtures of jarosite and goethite. The topographic relief, recent glaciation, dry cool climate, and geologic youth of the area have restricted chemical weathering to the very near surface environment.

REFERENCES CITED

- Barth, T. F. W., 1969, Feldspars: New York, N.Y., Wiley - Interscience, 261 p.
- Blanchard, R., 1968, Interpretation of leached outcrops: Univ. Nev., Nev. Bur. Mines, 196 p.
- Burbank, W. S. and Goddard, E. N., 1935, Fissure eruptions of the Independence Pass district, Sawatch Range, Colorado: Amer. Geophys. Union Trans. 16th Ann. Mtg., p. 321-325.
- Candee, C. R., 1971, The Geology of the Lincoln Gulch stock, Pitkin County, Colorado (abs.): Geol. Soc. Amer. Rocky Mtn. Sect., v. 3, no. 6, p. 372.
- _____, 1971b, The geology of the Lincoln Gulch stock, Pitkin County, Colorado: M.S. Thesis, Colo. School Mines, 86 p.
- Creasey, S. C., 1966, Hydrothermal alteration, in Geology of the porphyry copper deposits: Tucson, Ariz., Univ. Ariz. Press, p. 51-74.
- Cruson, M. G., 1972, Grizzly Peak cauldron complex, Sawatch Range Colorado (abs.): Geol. Soc. Amer. Cordillern Sect., v. 4, no. 3, p. 142.
- Garrels, R. M. and Christ, C. L., 1965, Solutions, minerals, and equilibria: New York, N.Y., Harper & Row, 450 p.
- Hawkes, H. E., 1957, Principles of geochemical prospecting: U. S. Geol. Surv. Bull. 1000-F, p. 225-355.
- _____ and Webb, J. S., 1962, Geochemistry in mineral exploration: New York, N.Y. and Evanston, Ill., Harper & Row, 415 p.
- Hemley, J. J. and Jones, W. R., 1964, Chemical aspects of hydrothermal alteration with emphasis on hydrogen metasomatism: Econ. Geol., v. 59, p. 538-569.
- Henderson, C., 1908, Colorado, in Mineral resources of the United States: U. S. Geol. Surv., p. 394.
- _____, 1911, Colorado, in Mineral resources of the United States: U. S. Geol. Surv., p. 556.
- _____, 1929, Gold, silver, copper, lead, and zinc in Colorado, in Mineral resources of the United States: U. S. Bur. Mines, p. 951.

- Hollister, O. J., 1867, The mines of Colorado: Springfield, Mass., S. Bowles & Co., 450 p.
- Howell, J. V., 1919, Geology and ore deposits of the Twin Lakes district of Colorado: Colo. Geol. Surv. Bull. 17, p. 108.
- Lipman, P., Mutschler, F. E. and Bryant, B., 1969, Similarity of cenozoic igneous activity in the San Juan and Elk Mountains, Colorado, and its regional significance: U. S. Geol. Surv. Prof. Paper 650-D, p. 33-42.
- MacKenzie, W. B., 1970, Hydrothermal alteration associated with the Urad and Henderson molybdenite deposits, Clear Creek County, Colorado: Ph.D. Thesis, Univ. Mich., 208 p.
- Meyer, C. and Hemley, J. J., 1967, Wall rock alteration, in Geochemistry of hydrothermal ore deposits: New York, N.Y., Holt, Rinehart and Winston, Inc., p. 166-232.
- Moorhouse, W. W., 1959, The study of rocks in thin section: New York, N.Y. and Evanston, Ill., Harper & Row, 514 p.
- Naramore, C., 1906, Colorado, in Mineral resources of the United States: U. S. Geol. Surv., p. 230.
- _____, 1907, Colorado, in Mineral resources of the United States: U. S. Geol. Surv., p. 268.
- Neville, A. M. and Kennedy, J. B., 1964, Basic statistical methods for engineers and scientists: Scranton, Pa., Internat. Textbook Co., 325 p.
- Obradovich, J. D., Mutschler, F. E. and Bryant, B., 1969, Potassium-argon ages bearing on the igneous and tectonic history of the Elk Mountains and vicinity, Colorado: A preliminary report: Geol. Soc. Amer. Bull., v. 80, p. 1749-1756.
- Stark, J. T. and Barnes, F. F., 1935, Geology of the Sawatch Range, Colorado: Colo. Sci. Soc. Proc., v. 13, no. 8, p. 467-479.
- Tweto, O., 1968, Geologic setting and interrelationships of mineral deposits in the Mountain Province of Colorado and south-central Wyoming, in Ore deposits in the United States, 1933-1967: New York, N.Y., A.I.M.E., p. 551-604.
- _____, and Sims, P. K., 1963, Precambrian ancestry of the Colorado mineral belt: Geol. Soc. Amer. Bull., v. 74, p. 991-1014.
- Turekian, K. K. and Wedepohl, K. H., 1961, Distribution of the elements in some major units of the earth's crust: Geol. Soc. Amer. Bull., v. 72, p. 175-192.
- Vanderwilt, J. W., 1947, ed., Mineral resources of Colorado: Colo., Mineral Res. Bd., 547 p.

_____ and Koschman, A. H., 1932, Geology of the Independence Pass district, Colorado (preliminary report): U. S. Geol. Surv. in cooperation with Colo. Metal Mining Fund, 10 p.

Vinogradov, A. P., 1962, Average contents of chemical elements in the principal types of igneous rocks of the earth's crust: Geokhimiya, no. 7, p. 555-571.

Wallace, S. R., Muncaster, N. K., Jonson, D. C., MacKenzie, W. B., Bookstrom, A. A. and Surface, V. E., 1968, Multiple intrusion and mineralization at Climax, Colorado, in Ore deposits in the United States, 1933-1967: New York, N.Y., A.I.M.E., p. 605-640.

TABLE VI
MAJOR ELEMENT ANALYSES¹

Sample No.	% CaO	% Na ₂ O	% K ₂ O	% MgO	% MnO	% Fe ₂ O ₃	% TiO ₂	% P ₂ O ₅	% Al ₂ O ₃	% SiO ₂
Quartz latite porphyry stock										
32 ²	0.028	0.52	6.10	0.40	0.005	1.00	0.19	0.13	13.3	74.0
25 ³	0.043	0.57	4.2	0.53	--	--	--	--	12.3	70.3
29 ³	0.027	0.16	6.6	0.51	--	--	--	--	13.4	72.5
45 ³	0.081	0.58	4.2	0.63	--	--	--	--	12.6	70.0
68 ³	0.018	0.13	7.1	0.45	--	--	--	--	14.0	70.5
Quartz latite porphyry dikes										
55 ³	1.9	3.6	4.1	0.77	--	--	--	--	14.2	70.8
17 ²	1.15	3.7	3.8	0.61	0.050	2.14	0.28	0.09	15.8	69.5
Rhyolite ash-flow tuff										
76 ²	0.85	2.8	5.0	0.23	0.052	1.22	0.19	0.06	13.1	73.5

¹By weight percent.

²Analyses by Rock Mountain Geochemical Corporation, Salt Lake City, Utah.

³Analyses by Skyline Labs, Inc., Wheat Ridge, Colorado.

TABLE VII
TRACE ELEMENT ANALYSES

Sample ¹ No.	Cu (ppm)	Pb (ppm)	Zn (ppm)	Mo ² (ppm)	W ² (ppm)
1	20	125	130	2	6
2	20	40	90	-2	-2
3	N	N	N	N	N
4	N	N	N	N	N
5	N	N	N	N	N
6	10	65	50	-2	12
7	5	15	65	-2	3
8	5	40	45	4	3
9	5	10	50	2	-2
10	130	65	280	3	2
11	15	560	710	105	12
12	25	115	160	5	5
13	N	N	N	N	N
14	15	35	130	4	-2
15	5	15	90	-2	2
16	60	10	70	4	2
17	15	10	55	-2	-2
18	5	10	10	2	4
19	50	5	10	140	16
20	30	15	10	130	25
21	30	25	15	12	5
22	N	N	N	N	N
23	30	25	5	53	7
24	35	100	45	2	3
25	45	5	5	30	4
26	20	55	5	4	4
27	65	35	15	31	5
28	50	10	10	19	2
29	30	40	5	30	8
30	95	25	10	7	3
31	110	55	10	280	38
32	N	N	N	N	N
33	5	20	60	8	-2
34	15	10	100	-2	-2
35	10	20	60	-2	2

TABLE VII (Continued)

Sample ¹ No.	Cu (ppm)	Pb (ppm)	Zn (ppm)	Mo ² (ppm)	W ² (ppm)
36	40	10	85	-2	-2
37	5	20	75	-2	-2
38	5	25	95	-2	8
39	15	5	45	-2	-2
40	15	10	20	2	-2
41	5	25	50	2	-2
42	5	15	80	2	-2
43	40	210	10	5	4
44	5	5	5	3	-2
45	65	35	15	95	7
46	20	15	95	3	-2
47	20	10	35	-2	-2
48	10	15	10	23	6
49	5	25	110	-2	-2
50	15	75	60	3	-2
51	20	60	300	3	-2
52	N	N	N	N	N
53	55	10	105	2	-2
54	15	35	115	5	-2
55	5	15	100	-2	2
56	25	55	60	2	2
57	5	10	45	2	2
58	180	5	25	-2	-2
59	-5	15	40	-2	-2
60	15	40	60	2	-2
61	5	-5	45	3	-2
62	5	5	190	6	-2
63	680	40	120	2	-2
64	5	30	110	2	3
65	95	20	40	2	2
66	15	35	10	2	5
67	1,000	15	80	2	2
68	25	40	15	110	6
69	35	40	5	48	8
70	25	25	5	38	8

TABLE VII (Continued)

Sample ¹ No.	Cu (ppm)	Pb (ppm)	Zn (ppm)	Mo ² (ppm)	W ² (ppm)
71	20	15	5	22	5
72	20	25	5	20	5
73	10	15	70	-2	3
74	70	30	25	-2	10
75	N	N	N	N	N
76	N	N	N	N	N

¹(N) denotes no analyses, see Figure 20.

²(-) denotes less than (x) ppm.

VITA

Mark John Holtzclaw

Candidate for the Degree of

Master of Science

Thesis: GEOLOGY, ALTERATION, AND MINERALIZATION OF THE RED MOUNTAIN
STOCK, GRIZZLY PEAK CAULDRON COMPLEX, COLORADO

Major Field: Geology

Biographical:

Personal Data: Born in Bozeman, Montana, September 22, 1948, the
son of Mr. and Mrs. John Edward Holtzclaw.

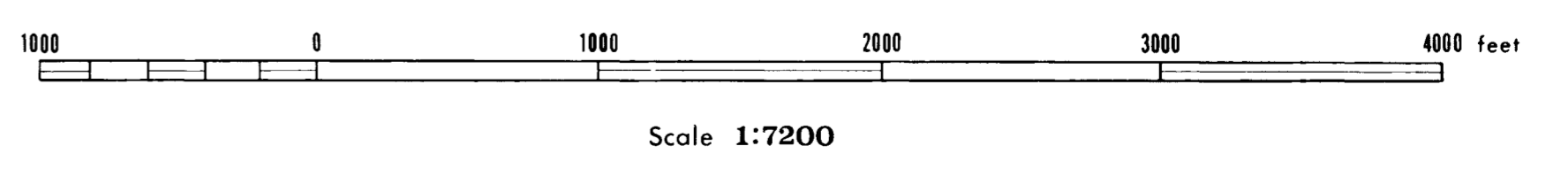
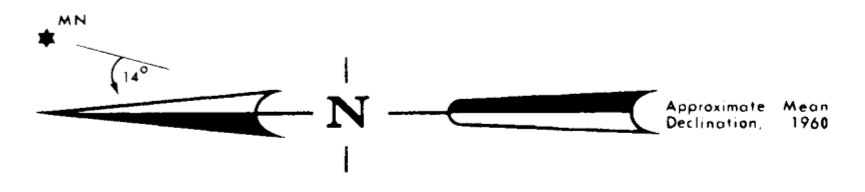
Education: Graduated from Alva High School, Alva, Oklahoma, in May,
1966; received the Bachelor of Science degree from Oklahoma
State University, Stillwater, Oklahoma in January, 1971, with a
major in Geology; completed requirements for the Master of
Science degree at Oklahoma State University in May, 1973, with
a major in Geology; nominated for membership in national honor
society, Phi Kappa Phi.

FIGURE 3
GEOLOGIC MAP OF THE RED MOUNTAIN AREA, GRIZZLY PEAK CAULDRON COMPLEX, COLORADO



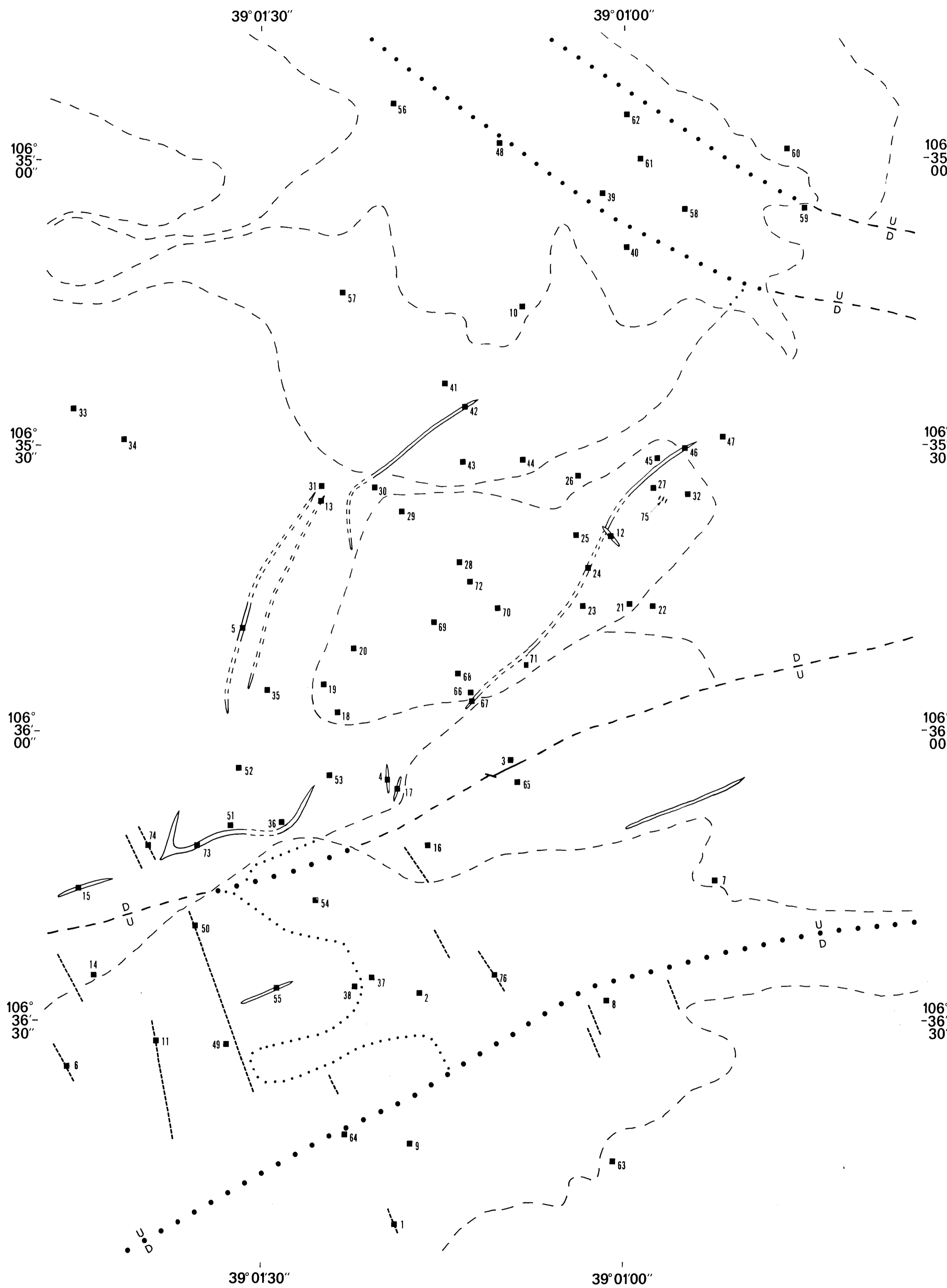
EXPLANATION

- | | | | | |
|-------------|------------|------------|---|-------------------|
| CENOZOIC | Quaternary | Qu | Alluvium, till, and rock glaciers undivided | |
| | Tertiary | Oligocene | Trp | Rhyolite porphyry |
| | | Tdp | Dacite porphyry | |
| | | Tib | Intrusive breccia | |
| | | Tqld | Quartz latite porphyry | |
| | | Tqlp | Quartz latite porphyry stock: outcrops shown | |
| | | Tap | Andesite porphyry | |
| PRECAMBRIAN | | Tgpr, Tgpb | Grizzly Peak volcanics
Tgpr - rhyolite ash-flow tuffs
Tgpb - slump breccias | |
| | | pCqm | Quartz biotite monzonite | |
| | | pCss | Sawatch Schist and Migmatite | |
-
- - - - - Contact, dashed where inferred, dotted where concealed
 - 70 - - - - Fault showing dip and relative displacement, dashed where inferred, dotted where concealed
 - 80 - - - - Mineralized fractures showing dip
 - 10 / \ Strike and dip of compactional layering in ash-flow tuffs
 - 78 / \ Strike and dip of foliation and/or lineation in metamorphic rocks
 - 88 / \ Strike and dip of joints
 - x □ Mine workings: adit, prospect pit, shaft
 - Buildings
 - - - - - Unimproved roads and trails
 - - - - - Perennial and intermittent streams
 - A - - - - Line of cross section



By
Mark John Holtzclaw
Oklahoma State University
1973

INDEX MAP TO SAMPLE LOCATIONS



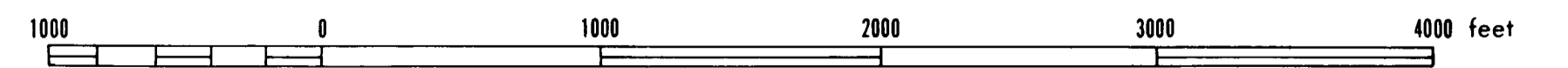
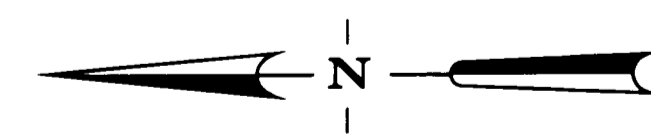
EXPLANATION

Faults and contacts are as shown on the geologic map (Fig. 3)

■ Sample location

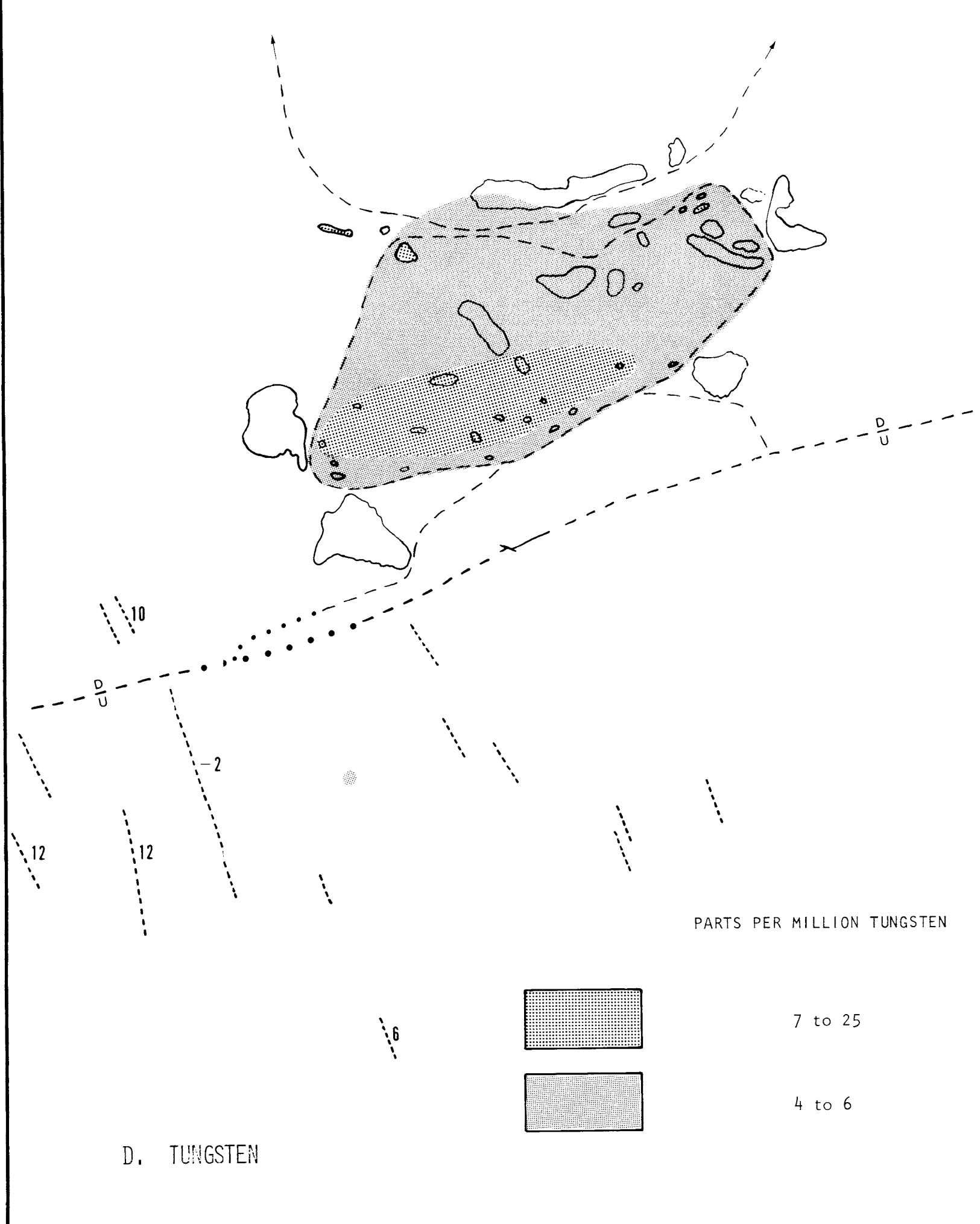
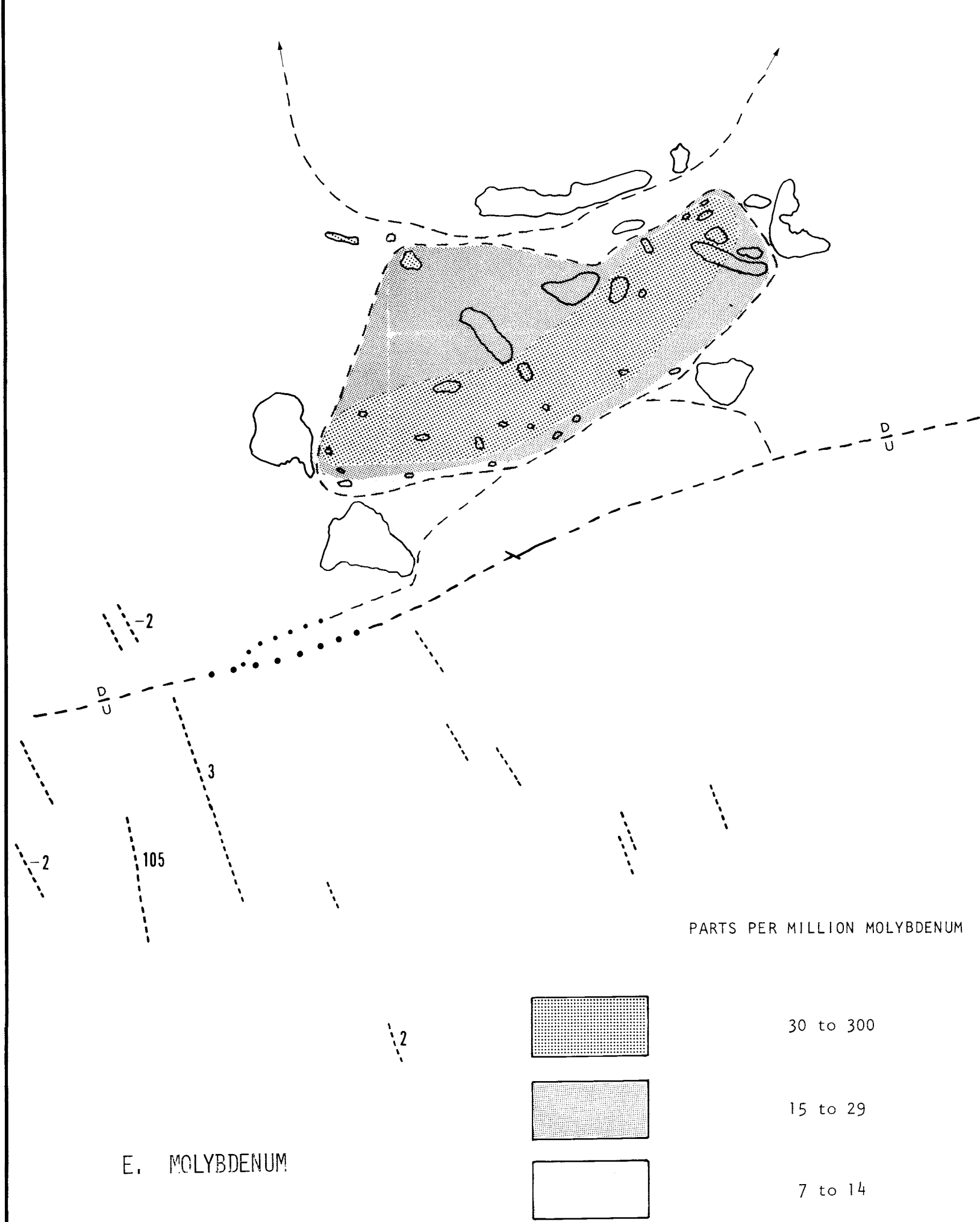
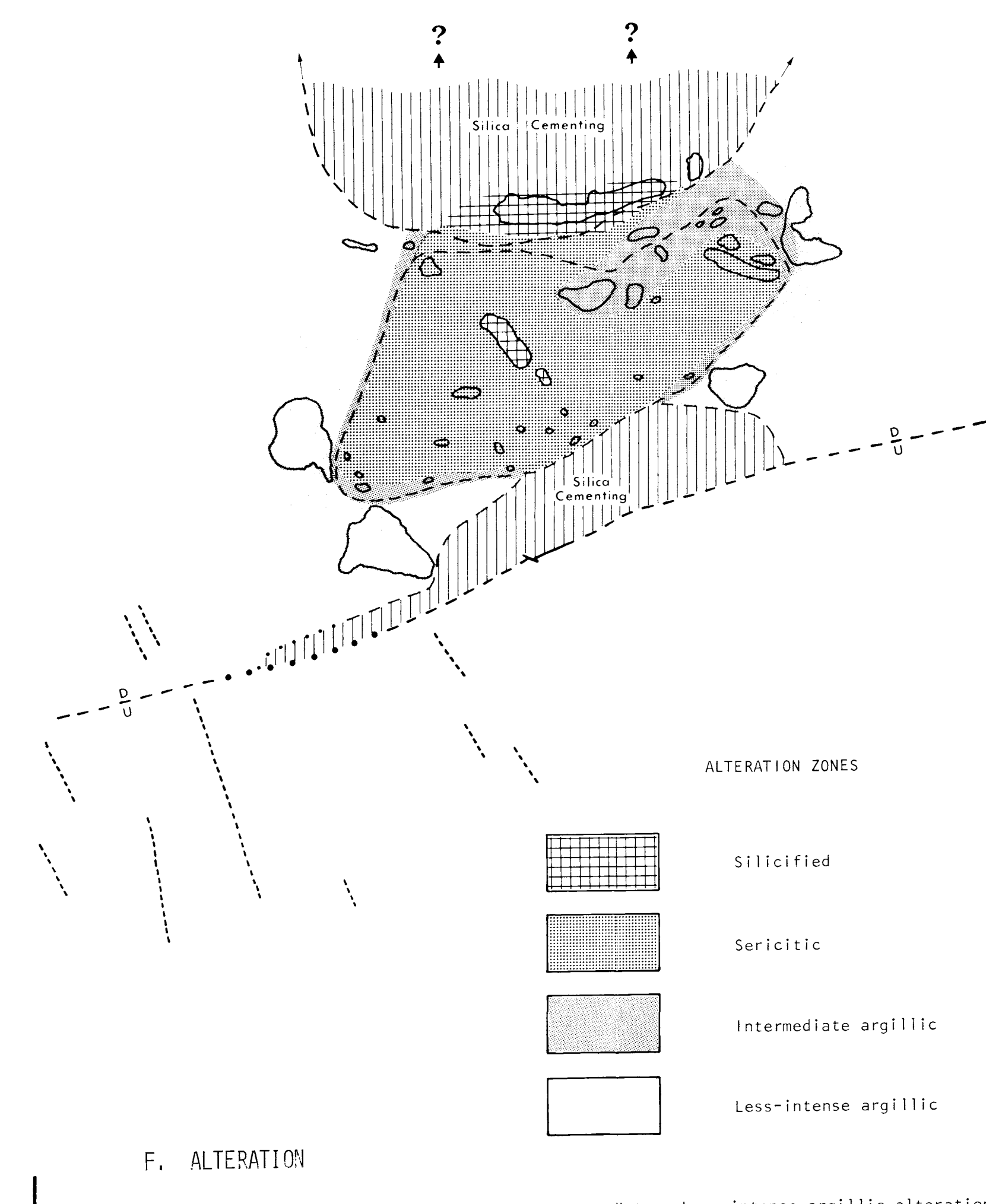
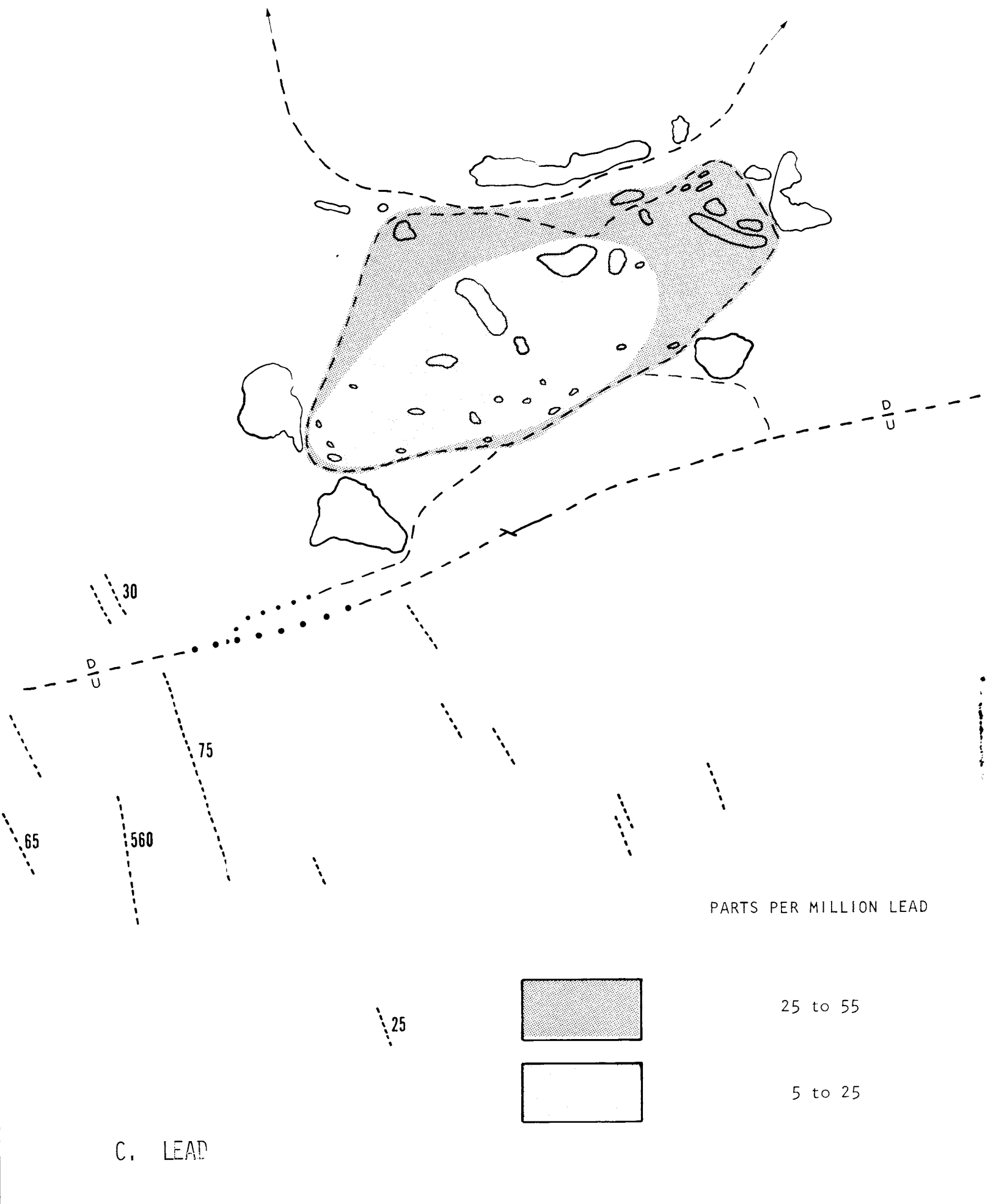
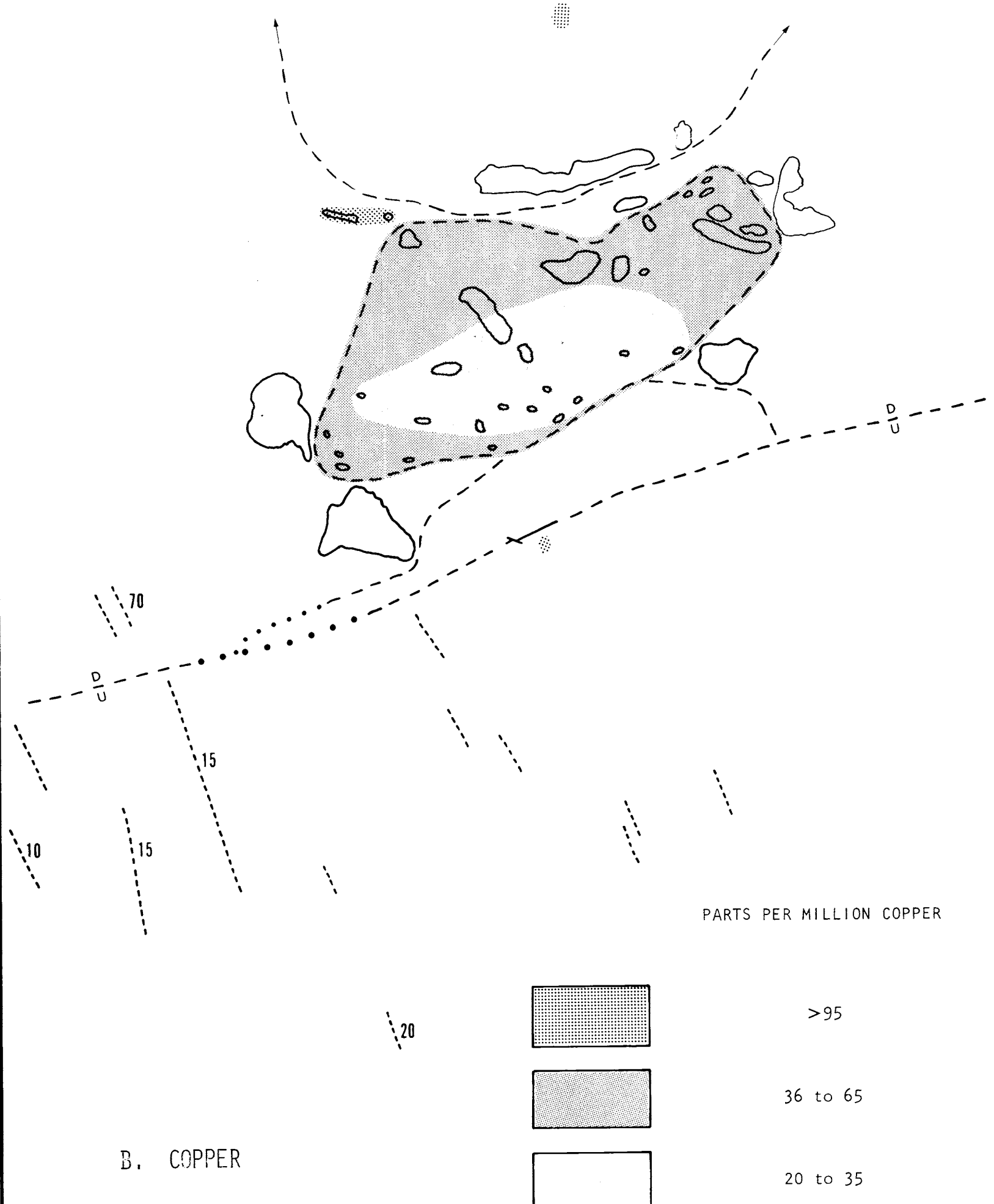
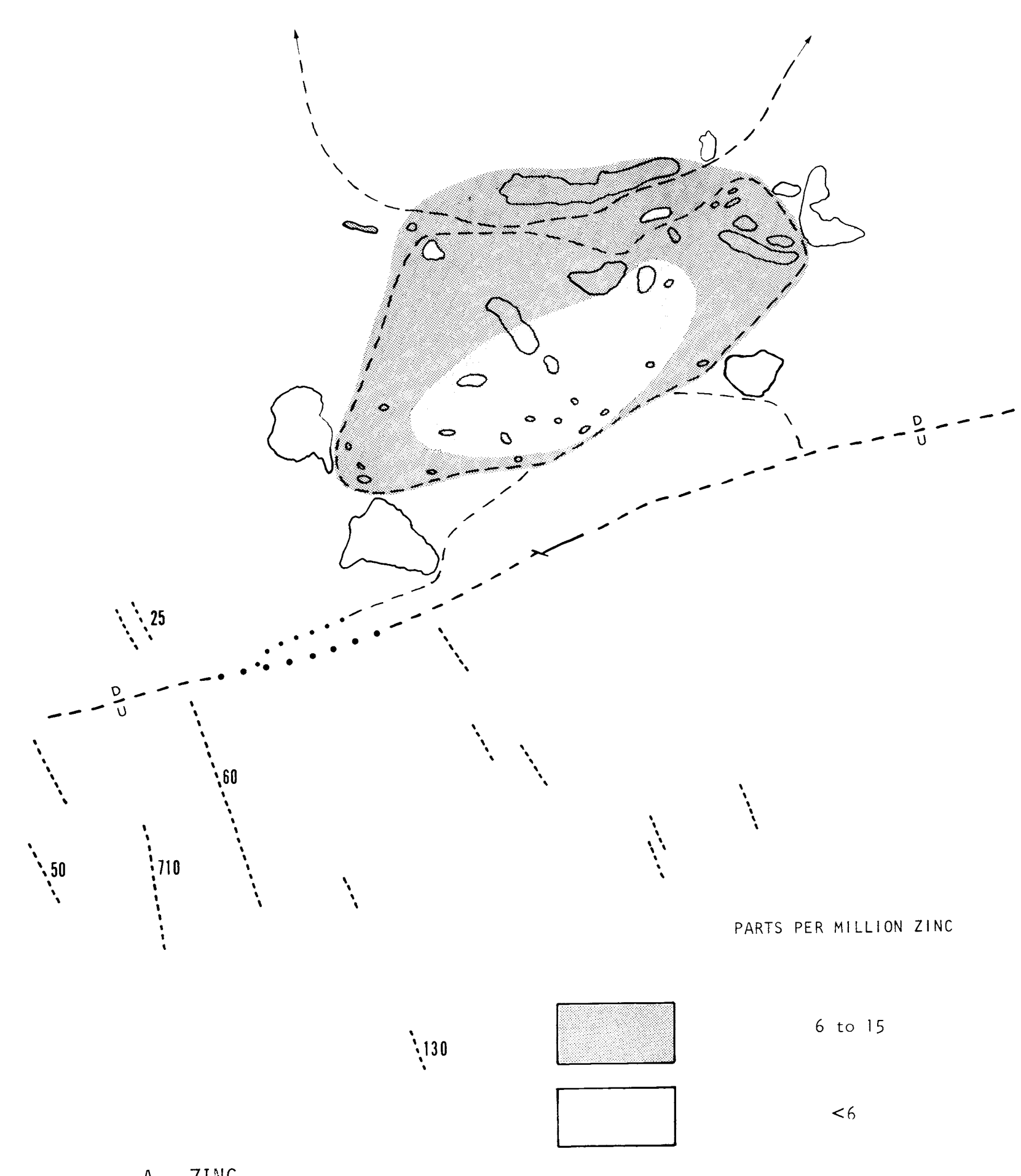
SAMPLE ANALYSIS

Sample No.	Trace Element	Major Element	Thin Section	X-ray Diffraction
1	X			
2	X			
3			X	
4			X	
5			X	
6	X			
7	X			
8	X			
9	X			
10	X			
11	X			
12	X		X	
13			X	
14	X		X	
15	X		X	
16	X			
17	X			
18	X	X	X	
19	X			X
20	X		X	X
21	X			X
22			X	
23	X			X
24	X		X	
25	X	X	X	X
26	X		X	
27	X			X
28	X			X
29	X	X	X	X
30	X		X	X
31	X		X	
32		X	X	X
33	X			
34	X		X	
35	X		X	X
36	X			
37	X			
38	X		X	
39	X			
40	X		X	
41	X			
42	X		X	
43	X		X	X
44	X		X	
45	X	X	X	X
46	X		X	
47	X		X	X
48	X			
49	X		X	
50	X			
51	X		X	
52			X	
53	X			X
54	X		X	
55	X	X	X	
56	X			
57	X		X	
58	X			
59	X		X	
60	X		X	
61	X		X	
62	X			
63	X		X	
64	X		X	
65	X			
66	X			
67	X		X	X
68	X	X	X	X
69	X			X
70	X		X	X
71	X			X
72	X		X	X
73	X		X	
74	X			
75		X	X	
76		X	X	



Scale 1:7200

By
Mark John Holtzclaw
Oklahoma State University
1973



OKLAHOMA
STATE UNIVERSITY
LIBRARY
OCT 19 1973

FIGURE 21
TRACE ELEMENT AND ALTERATION
DISTRIBUTION MAPS

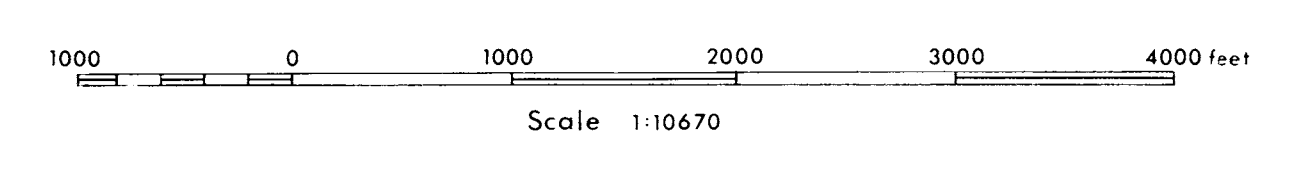
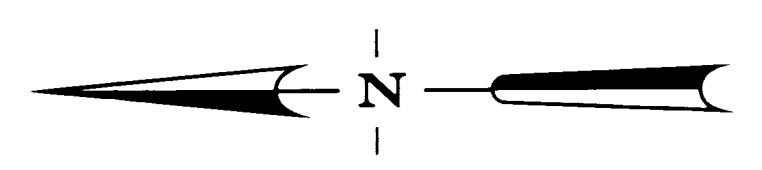
EXPLANATION

Faults, fractures, and contacts are as shown on the geologic map (Fig. 3)

Solid lines denote outcrops

Numerical values on trace element maps record the respective values in parts per million for samples collected along and/or within fractures; (-) indicates "less than" value (X)

Note: All trace element analyses were performed on rock-chip samples.



By
Mark John Holtzclaw
Oklahoma State University
1973